BACTERIOLOGICAL REVIEWS, Mar., 1965 Vol. 29, No. 1
 Printed in U.S.A.

Independent-Action and Birth-Death Models in Experimental Microbiology

GEORGE SHORTLEY AND JUDD R. WILKINS[1]

Booz, Allen Applied Research Inc., Bethesda, Maryland

INTRODUCTION

For many years, biologists have measured the infectiousness of microorganisms by recording the percentage of hosts that respond as a function of challenge dose (the quantal response). In studies on viruses and carcinogenic agents, the time interval between treatment of a host and the appearance of a detectable reaction has also been widely employed (the graded response). To evaluate quantal or graded responses efficiently, it is desirable to describe the relations between dose and response in mathematical terms. In this review, we describe and discuss two mathematical models: the independent-action model, which is concerned with the probability of response as a function of size of dose in quantal-response studies, and the birth-death model, which analyzes the distribution of response times as a function of dose in graded-response studies. The two models are consistent, and their joint use gives the capability of relating quantal and graded responses.

In this review, we discuss the simple-exponential response-probability function that follows from the independent-action assumption when hosts are homogeneous and receive identical treatment. Following a suggestion of Armitage (2), we show how host heterogeneity can be identified by plotting response percentages on a so-called Weibull scale. A representative group of experimental data was analyzed by the Weibull

[1] Present address: Eye Research Foundation of Bethesda, Bethesda, Md.

procedure, and effects of host age, host strain, and route of inoculation or response probabilities were examined. We concluded that the Weibull analysis of biological-response data is much more meaningful than the more common probit analysis, and will in many cases serve to divide the hosts into susceptible and resistant groups and give separate ID_{50} values for these groups. It is recommended that the Weibull type of analysis of response probabilities be more widely used.

In the section of this review dealing with the independent-action model, the only assumption made is that the organisms act independently. From this assumption alone, one can obtain information on the probability of response as a function of dose, but one can obtain no information on the distributions of time to response as a function of dose. To the independent-action assumption is added, in the section on the birth-death model, the simple assumptions of the "birth-death" model regarding the course of the infection. These assumptions are that, during the entire period before response, the conditions that govern the probabilities of organism fission (birth) and of organism death remain constant, independent of time and of the number of organisms. During this period, as a result of chance, either all organisms will disappear or the number of organisms will grow to a certain very large size, N, at which time response is assumed to occur with the appearance of an observable symptom. The mathematical treatment of this model of birth and death, in the papers by Saaty (50) and by Shortley (52), gives results that describe the frequency distribution of response times and its dependence on challenge dose; these results are quoted herein. Curves are given that show the predicted frequency distributions of time to response, the mean or average time to response, the standard deviations of the distributions and their skewnesses, all as functions of the size of initial challenge dose relative to the ID_{50}. It is shown how to analyze experimental data for comparison with the predictions and for determination of the basic parameters of the model.

The predictions of the birth-death model are compared with the experimental data in some detail. A comprehensive table is given that shows the exponential growth-rate parameters and the values of N for a large set of experimental data obtained by measuring average time to response as a function of dose. The effects of organism and site heterogeneity are then discussed, and it is shown that these effects are in general so significant that it is usually impossible to derive from the data meaningful individual values of λ, the growth probability per unit of time, and of μ, the death probability per unit of time, but that one can only obtain their difference, $\lambda - \mu$, which gives α, the average exponential growth rate. A comparison with naturally occurring respiratory disease in the case of Q fever is presented, and demonstrates that the natural disease results from a very minimal dose. It offers the hypothesis that other natural respiratory infections also result from minimal doses and that this fact accounts for the rather well-defined minimal incubation periods that are observed.

In conclusion, certain avenues of approach to the problem of identifying factors that influence susceptibility and resistance are suggested. Investigations of basic defense mechanisms associated with susceptibility in a heterogeneous host population are discussed. It is pointed out that the Weibull type of analysis in a heterogeneous population leads to the possibility of making individual host measurements prior to inoculation, carefully labeling the hosts and, after challenge, correlating the response with the measured host characteristics. Another approach to investigating basic defense mechanisms is based on the observation that young animals respond homogeneously and older ones heterogeneously, especially to viral diseases; research programs are suggested which involve correlating biochemical, physiological, and anatomical changes in the developing chick embryo with information about the pathogen, in an attempt to relate age with susceptibility. It is also suggested that tissue-culture systems be explored for their use in dose-response studies and as a tool for studying basic defense mechanisms.

INDEPENDENT-ACTION MODEL: PROBABILITIES OF RESPONSE

The predictions of the independent-action model have been occasionally, but not generally, used in the analysis of the probability of biological response as a function of size of dose.

After inoculation of a host with microorganisms (or viral particles), there is a period during which it is determined whether the number of particles is to grow to a large size, with a resulting response, or whether the organisms will all die, with no response. The independent-action model assumes that, during this "decision" period, the organisms (or viral particles) act independently of each other, each organism having a certain probability of causing infection. The total probability of infection from a given dose is then obtained by statistical combination of the probabilities for the individual organisms.

We shall describe in some detail the results of the independent-action assumption. We find that all of the data on biological-response probabilities, with the possible exception of certain

host-parasite systems requiring "overwhelming" doses to secure response, seem to be consistent with the hypothesis of independent action.

The first complete treatment of response probabilities under the assumption of independent action, with homogeneous and heterogeneous hosts and organisms, and with Poisson distribution of challenge-dose size about an expected dose d, was given by Fazekas de St. Groth and Moran (21). The basic formulas given below for response probability as a function of dose are derived from this work.

From the assumption of independent action it follows that, if all hosts are identical and receive identical treatment, there will be a definite median infectious dose (ID_{50}), which we call d_0, and a simple-exponential relation between the probability, R, of response and the expected dose, d:

$$R = 1 - e^{-0.69(d/d_0)} \text{ (homogeneous hosts)} \quad (1)$$

where $0.69 = \log_e 2$, the natural logarithm of 2. It is this factor that adjusts the exponent so that when $d = d_0$, $R = 0.5$, in accordance with the definition of d_0 as the dose required to infect 50% of a host population. In equation *1*, the dose d is the average dose given to a sample of hosts to determine the fraction of hosts responding. With the usual experimental technique, the actual dose will vary from host to host and have a Poisson distribution about the average dose d.

The simple-exponential form (*1*) applies whether or not the organisms are identical in strain or virulence and whether or not the organisms land at equally receptive sites in the host. All that is required for equation *1* to apply is that the hosts be identical and receive identical treatment.

A plot of equation *1*, with the fraction R on a percentage scale and d/d_0 on a linear scale, is given in Fig. 1. The same curve is plotted in Fig. 2 with the more usual logarithmic scale for d/d_0. Figure 2 also shows an example of data that conform excellently to the exponential dose-response relation. The data are from an experiment by Bang (3) on the probability of death of chick embryos injected with Newcastle disease virus. (The curve in Bang's Fig. 1, from which the data in our Fig. 2 are taken, is believed to be plotted "backward," with the longer tail at high doses rather than at low. This error has been corrected in our plot, to which the experimental data conform even more closely than in Bang's plot.) Confidence limits (50%) are shown in Fig. 2 and succeeding response plots. There is at most a 25% chance that the true response probability would be below the lower confidence limit and at most a 25% chance that it would be above the upper limit; there is at least a 50% chance that it would fall between these limits. A convenient table of these confidence limits is given in the Appendix of this review.

Figure 3 shows still a third way of plotting the curve given by equation *1*, this plot being on "probit" paper. Response probabilities are frequently plotted on the probit scale, with the curve of probit vs. log dose approximated by a straight line. The "probit slope" is defined as the increase in probit for each 10-fold increase in dose. As shown by the dashed tangent line in Fig. 3, the exponential response curve has a probit slope of 2.003 at the 50% response point.

Rather than using a probit scale, for which the response function (*1*) is actually a curved line, it is convenient to plot response probabilities on a scale, called the Weibull scale, for which the simple-exponential curve reduces to a straight line. This reduction is accomplished by

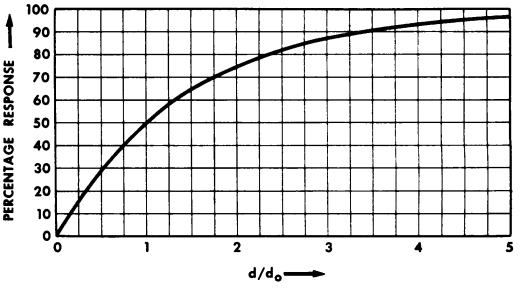

FIG. 1. *Exponential dose-response probability.*

plotting $\log_{10}[-\log_e(1 - R)]$ against dose (on a log scale), as in Fig. 4, which also shows the values of R itself on the left-hand scale. Figure 4 duplicates the curve and the data shown on Fig. 2.

The simple-exponential response-probability curve plots, on the Weibull scale of Fig. 4, as a straight line of such slope that the ordinate given by the right-hand scale increases by one unit for each 10-fold increase in dose. For example, for the straight line of Fig. 4, the ordinate increases from -1.16 at $d/d_0 = 0.1$ to -0.16 at $d/d_0 = 1$. We shall say that such a line has "unit slope."

Maximal Response Probability and Minimal Dose

Figure 5 shows another curve of response probability that indicates complete host homogeneity because it plots as a straight line of unit slope on the Weibull scale. The data in Fig. 5 refer to serological response to intraperitoneal

injection of *Coxiella burnetii* in guinea pigs, and are from a paper by Tigertt et al. (55).

In the similar plot of Fig. 4, the dosage scale is given as the ratio d/d_0, the actual numbers of virus "particles" being undetermined. In the case of Fig. 5, it was possible to count the rickettsial particles, at least approximately, and doses are given in numbers of organisms. The reference states that "the findings are compatible with the belief that . . . a single particle . . . is capable of initiating infection." Hence, the d_0 given by Tigertt et al. is 0.69 organisms, which is the average number of organisms in a quantity of inoculum that has, according to the Poisson distribution of actual numbers of organisms, exactly 50% probability of containing one or more organisms and 50% probability of containing no

faults in titration technique, or mistakes as to the cause of infection.

We should also point out that, while the form of the response curve in Fig. 5, where any single organism will cause response, is easily derived by computing the probability that the inoculum contains at least one organism, a response curve of the same form (a simple exponential) is obtained, as in Fig. 4, from the independent-action model for the case of a median infectious dose d_0 of any size whatsoever. One must not jump to the conclusion, as has been done occasionally in the viral literature [see, for example, references (12) and (44)], that, because a response in the form of a simple exponential function of d/d_0 is obtained, the virus is particulate in nature and a single virulent virus particle in the inoculum is certain

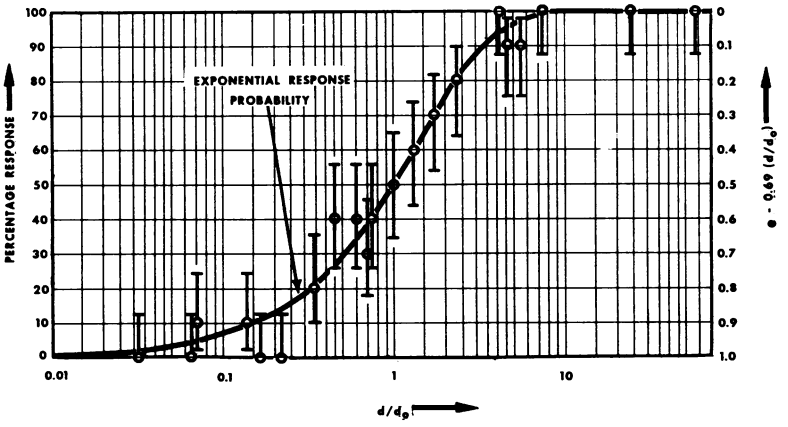

FIG. 2. *Percentage of deaths in chick embryos infected with Newcastle disease virus. Confidence limits (50%) are shown on this and succeeding figures.*

organisms. If any one inoculated organism causes infection, half the hosts will become infected when the average number of organisms in the inoculum is 0.69.

Furthermore, the straight line in Fig. 5, whose equation as a function of dose d is

$$R = 1 - e^{-0.69(d/0.69)} = 1 - e^{-d},$$

is just the probability that a quantity of inoculum, of average dose d, would contain at least one organism. Since at least one organism must be actually inoculated to cause infection, the response probability cannot be above this line under any assumption. We emphasize this statement because we occasionally find in the data impossible response probabilities, lying well above this curve. We also occasionally find values given for ID_{50} that are substantially below 0.69 organisms. Results of this type should be recognized to represent either errors in bioassay, to cause response. The conclusion that the exponential form is evidence of certainty of infection by any one particle is entirely erroneous.

Effect of Host Heterogeneity

If independent action is assumed, it can be shown that the only type of heterogeneity that can cause departures from the simple-exponential response-probability curve of Figs. 1 to 5 is heterogeneity among hosts. If all hosts are identical, there will be a definite median infectious dose (d_0) and an exponential dose-response function (*1*) no matter how heterogeneous the organisms may be in the inoculum or how heterogeneous may be the sites at which various organisms find themselves in the host—provided, of course, that the same inoculum is used for all hosts and that identical inoculation procedures are used.

If, however, the hosts differ in susceptibility,

such that a fraction α_1 of the hosts requires a median infectious dose d_1, a fraction α_2 requires d_2, a fraction α_3 requires d_3, etc., the response-probability formula corresponding to equation *1*

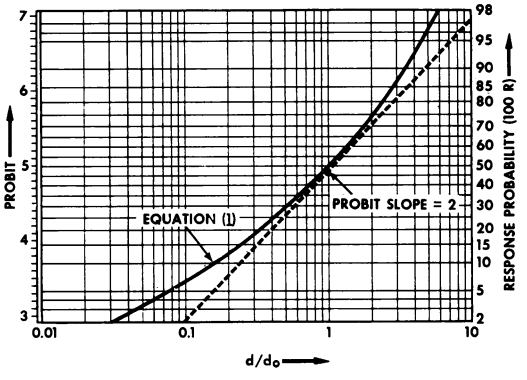

FIG. 3. *Exponential dose-response probability plotted on probit paper.*

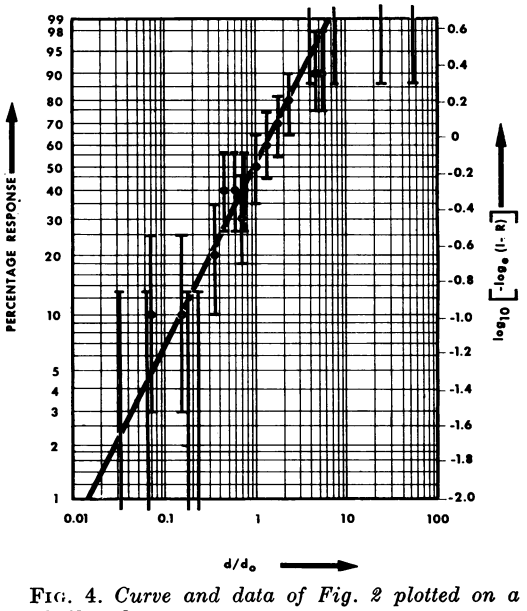

FIG. 4. *Curve and data of Fig. 2 plotted on a Weibull scale.*

becomes

$$R = 1 - \alpha_1 e^{-0.69(d/d_1)} - \alpha_2 e^{-0.69(d/d_2)} - \alpha_3 e^{-0.69(d/d_3)} - \cdots, \quad (2)$$

where, of course,

$$\alpha_1 + \alpha_2 + \alpha_3 + \cdots = 1. \quad (3)$$

Let us first illustrate the behavior of the complex relation (*2*) by a simple example in which the host population falls into just two groups, one highly susceptible and one highly resistant. Let us assume that 20% of the hosts have a median infectious dose of 1 organism, whereas the other 80% have a median infectious dose of 10^5 organisms; that is, we assume

$$\alpha_1 = 0.20, \quad d_1 = 1;$$
$$\alpha_2 = 0.80, \quad d_2 = 10^5.$$

The response probability is then

$$R = 1 - 0.2e^{-0.69(d/1)} - 0.8e^{-0.69(d/10^5)} \quad (4)$$

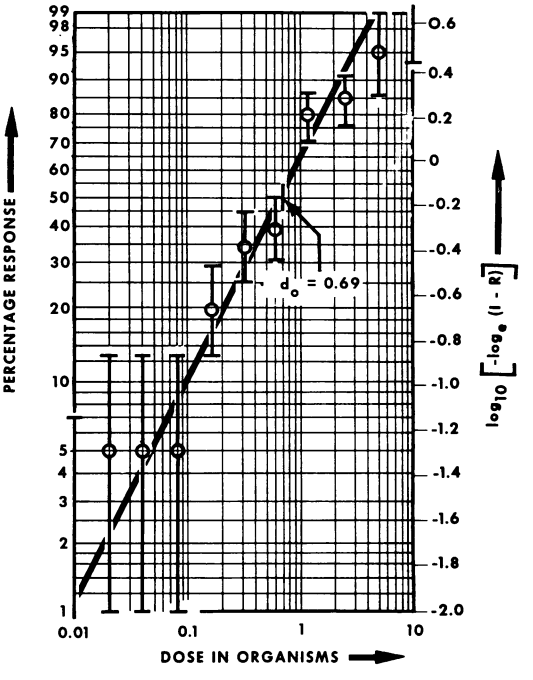

FIG. 5. *Percentage of serological responses in guinea pigs infected intraperitoneally with Coxiella burnetii.*

The values of R as a function of d are readily computed by reading the values of the exponentials from the right-hand scale of an accurate plot like that in Fig. 2. The resulting curve, plotted on a Weibull scale, has the form shown in Fig. 6.

If one finds a response-probability curve of the general form of that in Fig. 6, it is readily possible to work backward to estimate the values of the parameters α_1, α_2, d_1, and d_2. The following method was described by Armitage (2). We note first that there is a "shelf" at the 20% response level. The height of this shelf determines $\alpha_1 = 0.20$, the fraction of hosts that are "susceptible." We then find $\alpha_2 = 1 - \alpha_1 = 0.80$, the fraction of

"resistant" hosts. We notice next that at both high and low doses the curve becomes asymptotic to straight lines of the same slope as the straight line given in Fig. 4 for the simple-exponential response. From the points (marked by bars in Fig. 6) at which these straight lines cross the 50% response level, we can estimate d_1 and d_2. The value of d_2 is given directly by the bar on the right-hand asymptote, which is at $d_2 = 10^5$. The value of d_1 is not given directly by the bar on the left-hand asymptote. If we denote the position of the bar by d', we see that $d' = 5$ in Fig. 6. From the value d', the value of d_1 is determined by the relation $d_1 = \alpha_1 d' = 0.20 \times 5 = 1$ in our example.

We have been particularly struck by the large number of cases in which there is evidence of strong host heterogeneity but in which the hosts fall into just two groups, each with a clearly defined median infectious dose. As an example, we plot in Fig. 7 unpublished data, obtained from Ralph E. Lincoln, on percentage response to anthrax spores injected intraperitoneally in mice. These data fit excellently the response function

$$R = 1 - 0.65e^{-0.69(d/25)} - 0.35e^{-0.69(d/2.5\times10^4)} \quad (6)$$

which indicates that 65% of the hosts have

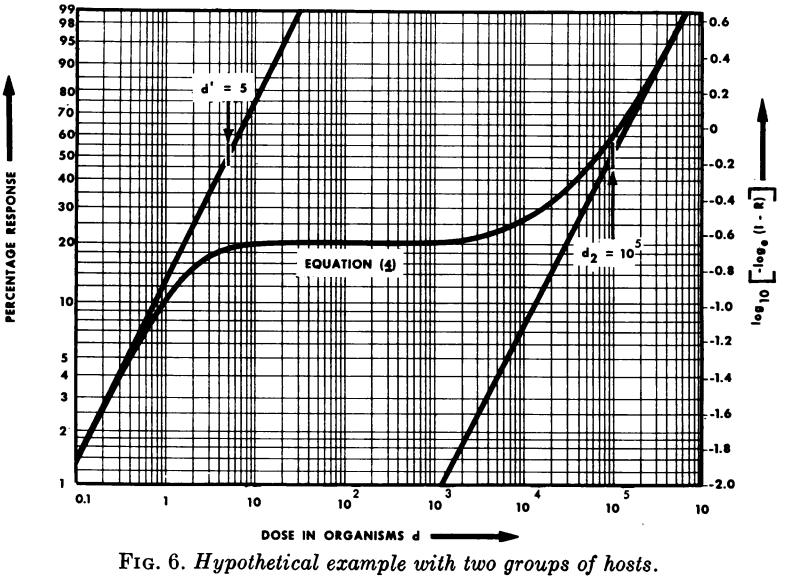

FIG. 6. *Hypothetical example with two groups of hosts.*

The above procedure is summarized as follows. (i) When the response-probability data, plotted on a Weibull scale, can be approximately represented by a shelf and two asymptotes of unit slope, the two-group formula

$$R = 1 - \alpha_1 e^{-0.69(d/d_1)} - \alpha_2 e^{-0.69(d/d_2)} \quad (5)$$

should be applicable. (ii) The value of α_1 is given by the response R at the height of the shelf. (iii) The value of α_2 is given by $1 - \alpha_1$. (iv) The value of d_2 is given by the dose at which the right-hand asymptote crosses the 50% response level. (v) If we denote by d' the dose at which the left-hand asymptote crosses the 50% response level, the value of d_1 is given by $d_1 = \alpha_1 d'$. (vi) As a final step, the curve (5) should be computed and plotted, and adjustments should be made in the parameter values if required to improve the fit to the data.

$d_1 = 25$ organisms, and the other 35% have $d_2 = 2.5 \times 10^4$ organisms.

Many laboratories have characteristically been subjecting their response data to a "probit" analysis. In a paper by Lincoln and DeArmon (35), the remark is made that, "In most of the quantal response bio-assays conducted in our laboratory, the average probit slope equals approximately 1.0 . . . Meynell claims that with an entirely uniform strain of animal the probit slope should approach 2.0." The last statement is only partially true. The line shown in Fig. 2, when plotted on probit paper, gives the curve of Fig. 3, which does not have the form of the straight line assumed in probit analysis, and which has the slope 2.0 only at the 50% point.

If the data of Fig. 7 are replotted on probit paper, we get the points shown on Fig. 8. If this plot is subjected to the usual probit analysis,

by use of a linear regression, we would find a probit slope of 0.7 and a median lethal dose of 250 organisms. However, the fit of the points to the straight line in Fig. 8 is not nearly so good as the fit to the curve in Fig. 7, and the evidence for two host groups is very strong, even in the departures of the observed points from the line in Fig. 8. If one accepts the two-group characterization, the median dose of 250 organisms does not characterize *any* of the individual hosts, but is merely a type of average characteristic of the way in which the population is distributed between sensitive and resistant hosts.

Our examination of a considerable body of response-probability data convinces us that the Weibull analysis (as in Fig. 7) is much more meaningful than probit analysis (as in Fig. 8),

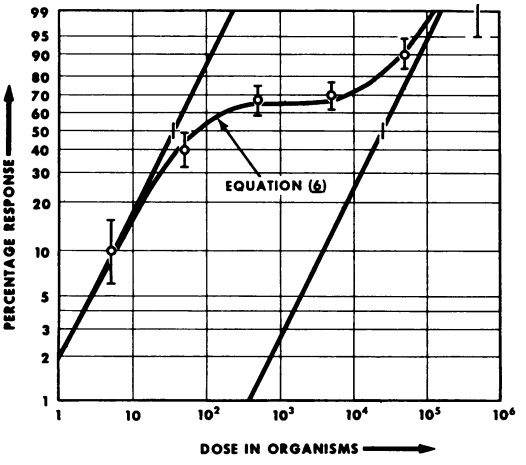

FIG. 7. *Percentage of deaths in mice infected intraperitoneally with Bacillus anthracis.*

and will in many cases serve to divide the hosts into groups and give separate ID_{50} values for these groups. It is strongly recommended that the Weibull type of analysis be more widely employed.

Figure 9 shows an example from Meynell and Meynell (40) of response data that cannot be fitted on the assumption that there are only two host groups; these data require three groups to get the satisfactory fit shown by the broken curve. It appears from an examination of these data that there are two shelves—one at about 11% response and one at about 60%—as indicated by the straight horizontal lines. We therefore assume that $\alpha_1 = 11\%$ of the hosts are highly susceptible, with $d_1 \leqq 10^2$ organisms (the position of the left asymptote is undetermined but we must have $d' \leqq 10^3$ and hence $d_1 = \alpha_1 d' \leqq 10^2$). The next group of hosts, comprising $\alpha_2 = 60 - 11 = 49\%$, would seem to have d_2 in the neighborhood of 2×10^6, the dose where the center slant line intersects the 50% response level. Finally, from the position of the right asymptote, we have $d_3 = 2 \times 10^7$ organisms for the most resistant group, comprising the remaining 40% of the hosts. As a trial, then, we take

$$\alpha_1 = 0.11, \quad \alpha_2 = 0.49, \quad \alpha_3 = 0.40,$$
$$d_1 \leqq 10^2, \quad d_2 = 2 \times 10^6, \quad d_3 = 2 \times 10^7,$$

and compute the response curve

$$R = 1 - 0.11e^{-0.69(d/d_1)} - 0.49e^{-0.69(d/210\times6)} - 0.40e^{-0.69(d/2\times10^7)} \quad (7)$$

This curve, shown by the broken line in Fig. 9, fits the data within the accuracy of the experiments except for the point at $d = 3 \times 10^6$,

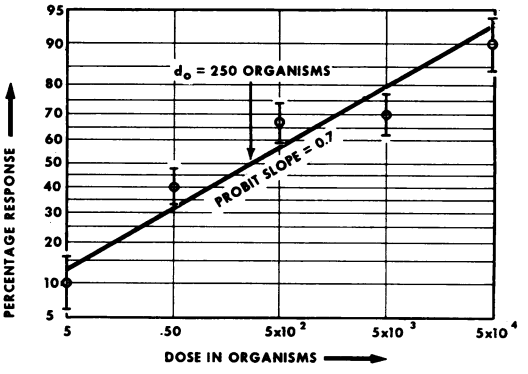

FIG. 8. *Probit response plot for the data of Fig. 7.*

which seems to be definitely inconsistent with the remainder of the data. The data of Fig. 9 would probably be equally consistent with the assumption that there are only two groups of hosts but that the resistant group is itself somewhat heterogeneous, with median lethal doses spread over a range from about 2×10^6 to 2×10^7.

For the data of Fig. 9, Meynell and Meynell give the median lethal dose as 3.2×10^6 organisms, a value which fairly well describes the resistant hosts but completely overlooks the definite existence of about 11% of much more sensitive hosts.

Demonstration of Host Heterogeneity

A very interesting experiment performed by Parker et al. (44) confirms the conclusion that departures from the simple-exponential response curve are an indication of host heterogeneity. In

this experiment, six rabbits were inoculated simultaneously with vaccinia virus, 10 inoculations being made in each rabbit with each dilution. For the pooled rabbits, the response (lesion) percentages are given in Fig. 10. The authors note that these data do not fit a simple-exponential curve. However, the authors showed that the data for each individual rabbit fit a simple-exponential curve with statistical significance. They found the rabbits to vary in susceptibility, and obtained the following log dilutions for the ID_{50} values for the six individual rabbits: -5.29, -5.13, -4.86, -4.84, -4.84, -3.49. The rabbits thus fall approximately into three groups: 33.3% with $d_1 = 10^{-5.21} = 6.2 \times 10^{-6}$; 50.0% with $d_2 = 10^{-4.85} = 1.4 \times 10^{-5}$; 16.7% with $d_3 = 10^{-3.49} = 3.2 \times 10^{-4}$. For this grouping, the overall dose-response probability is given by (see equation *2*):

$$R = 1 - 0.333e^{-0.69(d/6.2\times10^{-6})} - 0.500e^{-0.69(d/1.4\times10^{-5})} - 0.167e^{-0.69(d/3.2\times10^{-4})} \quad (8)$$

A plot of this curve gives the satisfactory agreement with the pooled data that is shown by the points on Fig. 10. Thus, in this case we are able to explain the complex character of the response-percentage curve by building it up from data on the individual hosts.

Continuous Distributions of Host Susceptibility

Response-probability curves are sometimes observed that could correspond to a continuous distribution of host susceptibility rather than to a clear-cut division into discrete groups. Figure 11 gives examples of the forms of the response curves that result when host susceptibility is continuously distributed. For curve A, the values of log d_0 are uniformly distributed over dose levels covering 1 log; for curve B, median doses are distributed over 2 logs; for curve C, over 3 logs. These distributions of median infectious dose are indicated at the bottom of the chart.

If x is the relative dose, and the log median infectious dose of the host population is uniformly distributed from log $x = 0$ to log $x = n$, corresponding to (nonuniform) distributions of the relative median infectious dose itself from $x = 1$ to $x = 10^n$, the response probability can

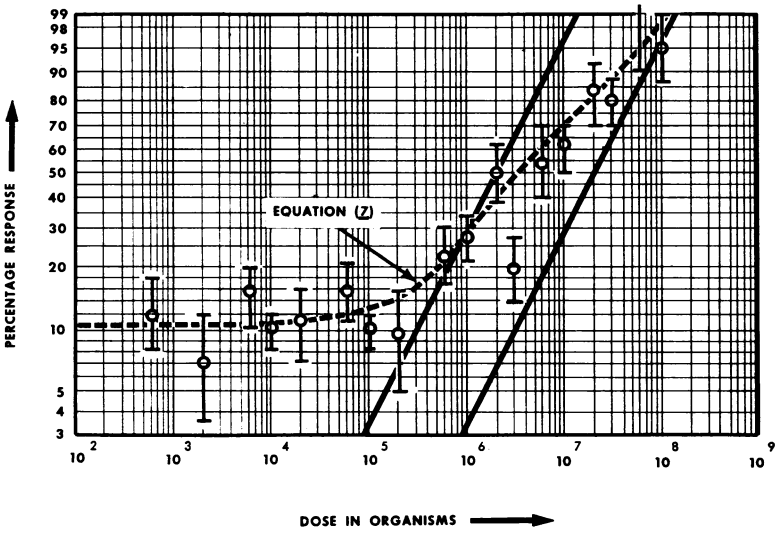

FIG. 9. *Percentage of deaths in mice infected intraperitoneally with Salmonella typhimurium. Experiments 2 and 3 of Meynell and Meynell (40).*

be computed from the formula

$$R = 1 - \frac{0.434}{n}[Ei(-0.693x) - Ei(-0.693 \times 10^{-n}x)], \quad (9)$$

where $0.434 = \log_{10} e$; $0.693 = \log_e 2$; and Ei is the logarithmic integral. The integral $Ei(-y)$ was tabulated by Jahnke, Emde, and Lösch in *Tables of Higher Functions* (p. 23) for values of y down to 0.01; for smaller values of y, one can use the approximation

$$Ei(-y) \approx \log_e y + 0.577 = 2.30 \log_{10} y + 0.577 \quad (10)$$

where 0.577 is Euler's constant.

A series representation of *9*, particularly useful

for small values of x, is

$$R = \frac{0.434}{n}\left\{(0.693x)(1 - 10^{-n}) - \frac{(0.693x)^2}{2\cdot 2!}(1 - 10^{-n})^2 + \frac{(0.693x)^3}{3\cdot 3!}(1 - 10^{-n})^3 - \cdots\right\}. \quad (11)$$

From the first term of this series, it can be shown that the left asymptote, indicated by a dashed line in Fig. 11, has unit slope and passes through the 50% ordinate at $x = n(1 - 10^{-n})/0.434$. For the cases $n = 1, 2, 3$, illustrated in Fig. 11, these

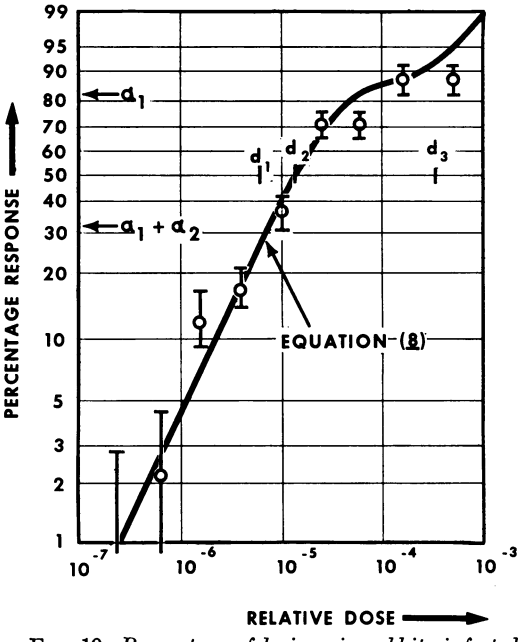

FIG. 10. *Percentage of lesions in rabbits infected intradermally with vaccinia virus.*

50% points for the asymptotes are at $x = 2.56$, 4.65, and 6.92, respectively, as indicated by the short bars.

Figure 12 gives an example, from work of Marshall and Gerone (39), of the type of data that can be represented by a continuous median-dose distribution, in this case extending over 3 logs. However, within the accuracy of the experiment, these data could as well be represented by two discrete groups and a shelf at about 65%. Because of the observed continuous increase of median dose with age, it is biologically reasonable to favor the continuous distribution in this case, as will be discussed later.

Effects with "Overwhelming" Doses

The nature of equations *2*,*9*, and others that correspond to different host-sensitivity distributions is such that the slope of the curve, when plotted on a Weibull scale, can never be greater than unity. This statement can be rigorously demonstrated. Occurrence of a part of the curve with greater than unit slope can only arise from cooperative, rather than independent, action.

In a few cases, we have observed dose-response curves which, on a Weibull plot, have slopes significantly greater than unity. Figure 13 shows an example from the work of Pike and Mackenzie (45) on *Salmonella typhimurium* injected intraperitoneally in a very homogeneous strain of Swiss mice. The agent was a TMO strain of low virulence. Blood counts and other evidence indicate that, with inoculations of 10^5 of fewer organisms, the count almost invariably decreases to zero after about 24 hr, whereas the number of organisms in inocula of 10^6 or more shows approximately the same growth pattern as a virulent strain that has median lethal dose of two organisms. In Fig. 13, there is a strong indication of a very steep rise in the region near 8×10^5 organisms. The evidence is strengthened by the fact that the experiments at 8×10^5 and at 10^6 organisms were performed with 50 animals each and have very narrow confidence limits.

In these experiments, there appears to be a critical dose below which the organisms cannot grow, but above which the organisms have normal virulence, with growth to a total of approximately 10^9 to 10^{10} organisms at death. Such a situation would not, of course, represent independent action, and one would not expect response probabilities in agreement with the independent-action model. Perhaps host defenses are "overwhelmed" by the large number of organisms in the inoculum, or by some toxic characteristic in the inoculum. It is noted that response probabilities for toxic chemicals characteristically give curves with slopes much steeper than those for biological agents.

Influence of Various Factors on Response Probabilities

This section will give examples of the dose dependence of observed response probabilities, and show how host response may be influenced by route of inoculation, host strain, age of host, and pathogen strain.

All of the curves in this section are fit-of-eye approximations. Ideally, these curves should be accurately computed and plotted, and adjustments should be made in the parameter values if required to improve the fit to the data. However,

for the purpose of demonstrating the effects of various factors on dose response, even a rough fit of the independent-action model is usually adequate. Confidence limits (50%) are shown along with the data points.

Route of inoculation. The study by Dutton (17) is the source of data for the following analysis of the effect of route of inoculation on response probabilities. In Dutton's study, albino mice of the Parker strain were inoculated intraperitoneally, subcutaneously, and intravenously geneous. Although the dose-response data are meager, the LD_{50} was estimated to be about two organisms by either route, a value close to the minimum possible. However, for mice challenged via the intravenous route, Fig. 16 shows a quite different behavior, in that the hosts clearly fall into two groups. A shelf extending across about 4 logs is apparent at about the 55% level. Approximately 55% of the hosts are susceptible, with d_1 of about 50 cells. The position of the upper asymptote gives a value of d_2 of about

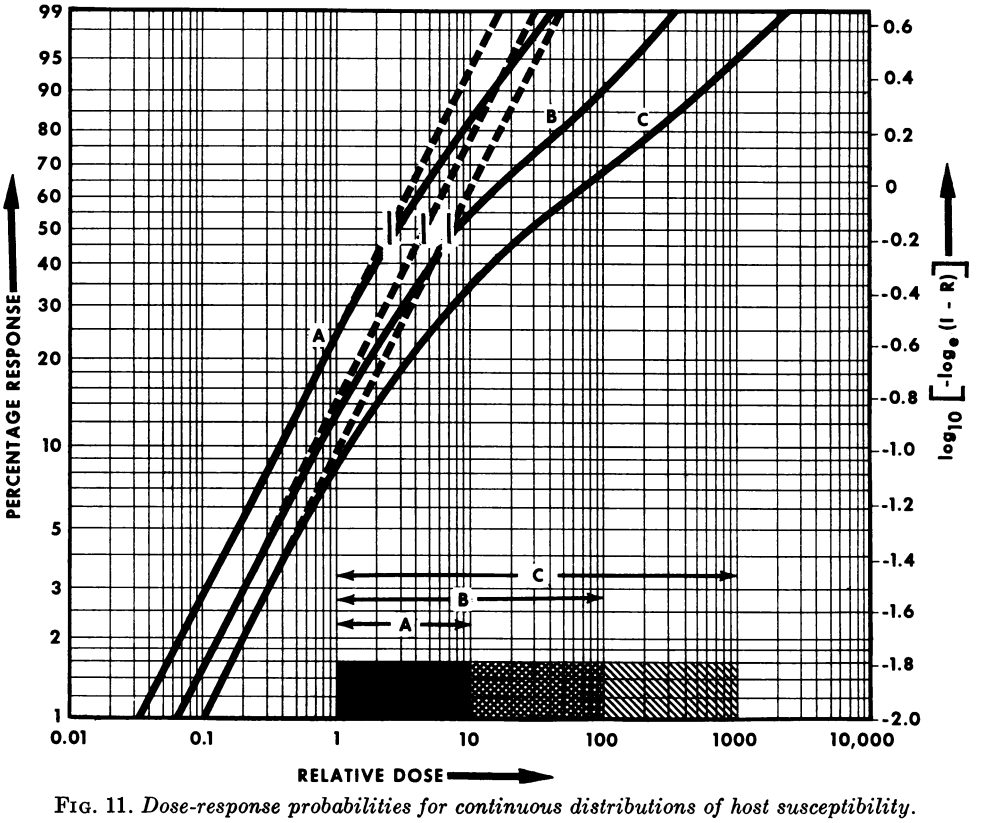

FIG. 11. *Dose-response probabilities for continuous distributions of host susceptibility.*

with eight genera of pathogenic bacteria. In most cases, 10 mice were used for each dose level and each route, and mortality percentages were recorded. For five of the organisms, the LD_{50} data, obtained by the methods previously described, are summarized in Table 1.

As an example, the plots of mortality percentages for *Streptococcus pneumoniae* inoculated by the three routes are presented in Fig. 14 to 16. When mice were challenged by either the intraperitoneal or subcutaneous routes, *S. pneumoniae* was very lethal. Figures 14 and 15 indicate that the host was extremely sensitive and homo-

8×10^5 organisms for the 45% of hosts that are resistant. These results are not open to an obvious explanation; one can only speculate as to possible mechanisms of action.

For all of the agents except *S. pyogenes*, the host reactions to subcutaneous inoculation are very similar to the reactions to intraperitoneal inoculations, but, in the case of *S. pneumoniae* and *S. typhimurium*, the reactions to intravenous inoculation are very different from these (Table 1).

Dutton's data demonstrates not only that the route of challenge can strongly influence the

median lethal dose, but that hosts that respond homogeneously to challenge by one route can respond very heterogeneously to challenge by another.

Host strain. Various host factors might be expected to influence the character of the response to a given organism. We shall give here an example illustrating the effect of strain of host, and in the next section we shall consider the effect of age of host.

A good example of the effect of host strain is included in the work of Pike and Mackenzie (45). These authors studied the same strain of *S. typhimurium* inoculated intraperitoneally in two strains of mice: one pure-bred and expected

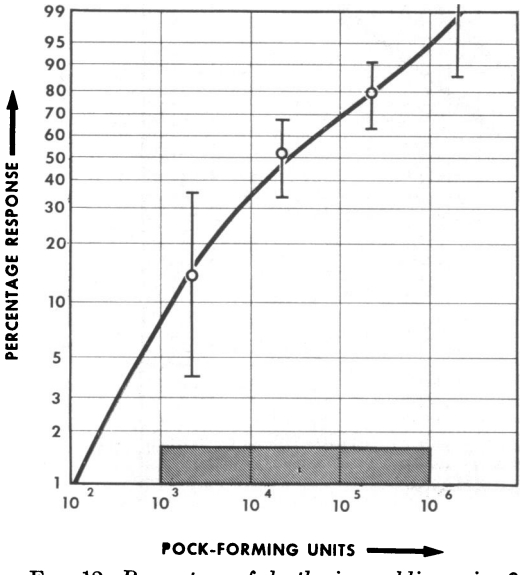

FIG. 12. *Percentage of deaths in suckling mice 3 to 5 days old infected intraperitoneally with variola virus.*

to react homogenously; the other deliberately crossed to obtain possible heterogeneity. The results obtained were exactly as anticipated.

The pure-bred Swiss mice were obtained from a breeder who maintained a large inbred colony. The other strain was obtained by crossing a Swiss doe with a wild brown buck and breeding the offspring with Swiss mice. The white offspring were inbred for two generations.

The mortality percentages are summarized in Table 2. Plots of the mortality data are presented in Fig. 17 and 18. The response of the pure-bred Swiss mice was at least 99% homogeneous. These mice were highly susceptible, with $d_0 \sim 3$ organisms (Fig. 17). On the other hand, the response of the Swiss-brown cross was heterogeneous, with 60% of the hosts having a $d_1 \sim 6$ organisms and 40% having a $d_2 \sim$ 40,000 organisms (Fig. 18).

This experiment illustrates that the deliberate introduction of a genetic host heterogeneity can result in strong response heterogeneity. The evidence indicates that the hosts fall into two clear-cut groups. Why, in this and many other cases, one finds just two levels of susceptibility, rather than a more continuous distribution, remains unexplained.

Age of host. It has been known for some time that age of the host at the time of challenge markedly influences response. We shall give two examples from the literature which show that the characteristic increase in resistance with

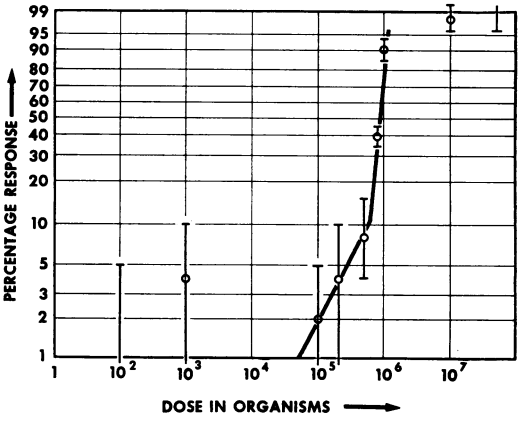

FIG. 13. *Percentage of deaths in Swiss mice infected intraperitoneally with Salmonella typhimurium of low virulence.*

age is generally accompanied by a marked heterogeneity of response during the transition period.

The above-mentioned heterogeneity is conspicuous for extraneural inoculation of certain neurotropic viruses in mice; in these instances, young suckling mice are very susceptible and older mice are resistant. In a carefully designed study, Lennette and Koprowski (33) determined the manner in which age influences the susceptibility of mice to infection with nine neurotropic viruses. In this study, albino Swiss mice of various ages were challenged by the intraperitoneal and intracerebral routes. For both routes, mice of various ages were inoculated with the same virus preparation. Each virus dilution was tested in a group of six mice. In many cases, more than one such group was tested at each dose level. Death was the recorded end point.

Mice of all ages were found to be very sensitive to intracerebral challenge of all neurotropic

viruses, and there was no significant diminution of sensitivity with increasing age.

In contrast, sensitivity to intraperitoneal inoculation was found to decrease strongly with age for the five viruses listed in Table 3. In the case of Venezeulan equine encephalomyelitis, the mice remained very sensitive to intraperitoneal challenge at all ages. For the five cases where age sensitivity was observed, Table 3 gives the percentage of hosts having various median lethal doses; these percentages were quired median dose. At 21 and 28 days of age, host heterogeneity was very evident, but with an increasing percentage of the animals becoming very resistant. By the age of 42 days, the mice were all very resistant to the virus. The general pattern of host response established by St. Louis encephalitis virus is also observed for the other viruses. When the hosts were inoculated intraperitoneally with West Nile and Japanese B encephalitis viruses, the departure from homogeneity came when the hosts were 21 days

TABLE 1. *Effect of route of inoculation on median lethal dose for various pathogenic bacteria*

Organism	Route of inoculation		
	Intraperitoneal	Subcutaneous	Intravenous
Streptococcus pneumoniae	Homogeneous $d_0 \sim 2$	Homogeneous $d_0 \sim 2$	55%, $d_1 \sim 50$ 45%, $d_2 \sim 800{,}000$
Streptococcus pyogenes	Homogeneous $d_0 \sim 300$	25%, $d_1 \leq 10$ 75%, $d_2 \sim 4{,}000$	Homogeneous $d_0 \sim 500$
Salmonella typhimurium	50%, $d_1 \sim 1{,}000$ 50%, $d_2 \sim 300{,}000$	30%, $d_1 \sim 600$ 70%, $d_2 \sim 200{,}000$	Very resistant $d_0 > 10^6$
Bacillus anthracis	80%, $d_1 \sim 40$ 20%, $d_2 \sim 8{,}000$	80%, $d_1 \sim 8$ 20%, $d_2 \sim 1{,}000$	95%, $d_1 \sim 60$ 5%, $d_2 \sim 2{,}000$
Erysipelothrix rhusiopathiae	50%, $d_1 \sim 10$ 50%, $d_2 \sim 3{,}000$	35%, $d_1 \leq 10$ 65%, $d_2 \sim 600$	30%, $d_1 \leq 10$ 70%, $d_2 \sim 800$

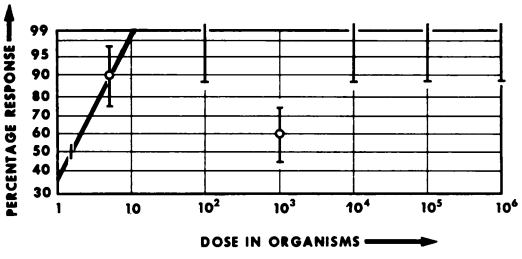

FIG. 14. *Percentage of deaths in mice infected intraperitoneally with Streptococcus pneumoniae. (Compare with Fig. 15 and 16.)*

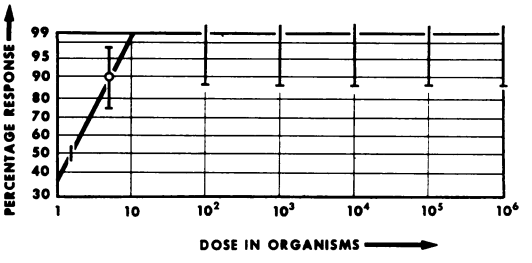

FIG. 15. *Percentage of deaths in mice infected subcutaneously with Streptococcus pneumoniae. (Compare with Fig. 14 and 16.)*

obtained from Weibull plots like that shown in Fig. 19.

In all cases, 8-day-old mice were highly susceptible and gave a homogeneous response when challenged by the intraperitoneal route with neurotropic viruses. Depending on the particular virus, host heterogeneity appeared at 14, 21, or 28 days of age.

In the case of St. Louis encephalitis virus, host heterogeneity appeared when the mice were 14 days of age, at which age 75% of the animals had developed a 3-log increase in re- old (Fig. 19). For Western and Eastern equine encephalomyelitis, host heterogeneity appeared at 28 days of age.

The data presented here clearly indicate the influence of age on host homogeneity or heterogeneity with neurotropic viruses, and show the shift to a high percentage of resistant animals with increasing age. Finally, this analysis offers an explanation for Lennette and Koprowski's statement that, "with increasing age death occurred so irregularly that calculation of a 50-percent end point was not warranted, or if cal-

culated, its accuracy was questioned." The explanation for this statement rests with the fact that, with increasing age, the hosts become heterogeneous and divide into two groups, one susceptible and one resistant. The determination of the LD_{50} for this type of data by any of the conventional techniques, e.g., the Reed and Muench or probit techniques, which do not identify host heterogeneity, is probably of little value.

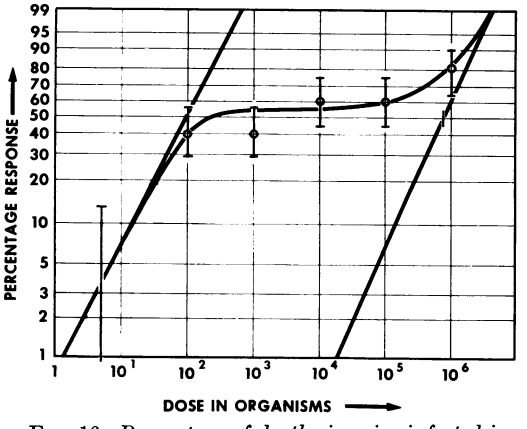

FIG. 16. *Percentage of deaths in mice infected intravenously with Streptococcus pneumoniae. (Compare with Fig. 14 and 15.)*

TABLE 2. *Mortality percentages of mice after intraperitoneal injection of Salmonella typhimurium*

Strain of mice	Dose (organisms)	No. of animals	Per cent mortality
Swiss	7	25	84
	10^2	25	100
	10^3	250	98.5
	10^5	25	100
	10^7	25	100
Swiss-brown cross	10	25	40
	10^3	50	62
	10^5	50	92
	10^6	25	100

Another example of the influence of host age on response is found in the studies by Roessler et al. (49) on the virulence of *Coccidioides immitis* inoculated by the yolk-sac route in embryonated eggs. The percentage mortalities for embryos of various ages are summarized in Table 4.

Two sets of data are given in Table 4 for 8-day hosts. The first set is from the same titration as the data for hosts of other ages. The second set is from a different titration of the same parent inoculum and should be directly comparable with the other 8-day data. Both sets of data are plotted in Fig. 20, and the combined data were used in the Wibull median-dose determination.

Table 4 shows a rapid increase of median lethal dose as the hosts age from 6 to 9 days. The host response is essentially homogeneous, except for 8-day hosts. Remarkably, at 8 days of age, about 20% of the hosts develop a specific sensitivity such that, to a good approximation, any one organism in the inoculum will cause death. One would suspect the validity of this conclusion were it not indicated by each titration independently, as well as by the combined 8-day data.

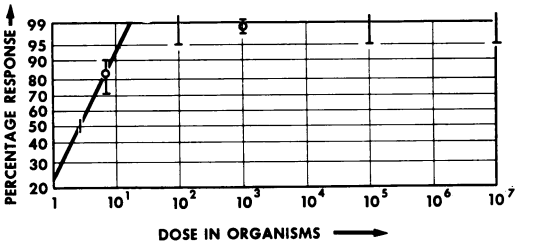

FIG. 17. *Percentage of deaths in Swiss mice infected intraperitoneally with Salmonella typhimurium. (Compare with Fig. 18.)*

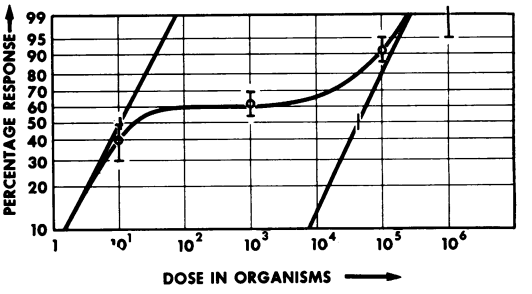

FIG. 18. *Percentage of deaths in Swiss-brown-cross mice infected intraperitoneally with Salmonella typhimurium. (Compare with Fig. 17.)*

It is suggested that the specific sensitivity indicated by these data of Roessler et al. be subjected to additional verification. If found to be correct, embryologists may be able to find clues, from the embryo-development pattern, as to the particular host factor that causes this sensitivity.

Pathogen strain. The strain of pathogen frequently influences the character of response-probability functions. As an example, the study of Donovan et al. (16) compares the response of guinea pigs to encapsulated and nonencapsu-

lated strains of *Pasteurella pestis*. In this study, the virulent MP-6 strain and its nonencapsulated mutant strain M-23, grown under similar conditions, were inoculated intradermally in the flanks of Hartley-strain guinea pigs, with the lethal response summarized in Table 5.

Plots of the data in Table 5 are given in Fig. 21 and 22. In general, the MP-6 encapsulated strain is more virulent than the M-23 when injected by the intradermal route in guinea pigs. As shown in Fig. 21, the guinea pigs were homogeneously sensitive to the MP-6 strain, with $d_c \sim 3$ organisms. In contrast, in response to the nonencapsulated M-23 strain, the hosts divided into two groups as shown in Fig. 22; 35% were sensitive with $d_1 \sim 20$ organisms and 65% were resistant with $d_2 > 2 \times 10^5$ organisms. Using the Litchfield and Wilcoxon method, Donovan et al. estimated the LD_{50} for the MP-6 strain as 1.2 organisms and for the M-23 strain as 4,500 organisms.

TABLE 3. *Influence of age on the response of mice to intraperitoneal challenge with certain neurotropic viruses*

Age (days)	Virus	Median lethal dose expressed in terms of dilution								
		10^{-9}–10^{-8}	10^{-8}–10^{-7}	10^{-7}–10^{-6}	10^{-6}–10^{-5}	10^{-5}–10^{-4}	10^{-4}–10^{-3}	10^{-3}–10^{-2}	10^{-2}–10^{-1}	$>10^{-1}$
8	St. Louis	100*								
14	encephalitis	25			75					
21						65				35
28								20		80
42										100
8	West Nile		100							
14	virus		100							
21			55				45			
28					20				80	
42					40					60
8	Japanese B	100								
14	encephalitis	100								
21			80					20		
28				50					50	
42						25				75
8	Western equine	100								
14	encephalo-		100							
21	myelitis		100							
28				40				60		
42				55					45	
8	Eastern equine	100								
14	encephalo-		100							
21	myelitis				100					
28						40		60		
42							30		70	
56									100	
200									100	

* Percentage of hosts with indicated lethal doses.

Validity of the Exponential Response-Probability Function

Aside from a few cases that seem to depend on cooperative action with overwhelming doses of an organism of low virulence, such as the case discussed in connection with Fig. 13, all of the data we have examined are consistent with the independent-action model. The response-probability curve is either a simple exponential, a two-group exponential, or a more complex shape, but never has slope greater than unity when plotted on a Weibull scale. This statement applies to inoculations by all appropriate routes. It applies to responses of all types, including the growth of warts and tumors. It applies not only to infections by viral agents, rickettsia, and bacteria,

but to mycotic agents, tumor cells, and trypanosomes. It applies to all types of hosts, including tissue cultures.

We have found many response-probability curves that closely approximate the simple-exponential form, indicating complete or almost complete host homogeneity. Where heterogeneity is apparent, the hosts are divided, in a remarkable number of cases, into just two groups, as illustrated by various examples in this review. One case of an apparently continuous distribution of sensitivity, already illustrated in Fig. 12, occurs in the experiments of Marshall and Gerone (39) on intraperitoneal inoculation of variola virus in suckling mice. Newborn mice are highly susceptible, but gradually lose this susceptibility and become increasingly resistant during the first week. The data on response percentages within

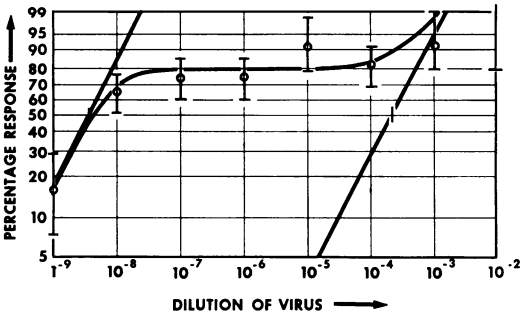

FIG. 19. *Percentage of deaths in 21-day-old mice infected intraperitoneally with Japanese B encephalitis virus.*

each age group can be interpreted as a continuous distribution of LD_{50} with a spread of about 3 logs, with the range of the LD_{50} distribution (given in pock-forming units) moving to larger doses as the age increases, as indicated in Table 6. The response data for the third group in Table 6 were plotted in Fig. 12.

One very exceptional response-probability curve was found by Eckert et al. (18) for the intravenous inoculation of the virus of avian erythromyeloblastic leukosis in chickens, the response being the appearance of primitive cells in the blood. The curve of response probability versus dose is extraordinarily flat, the probability increasing regularly with increasing dose but requiring about 6 logs to increase from 20 to 80%. This behavior has not been satisfactorily explained; on the independent-action model, it would indicate a continuous distribution of host susceptibility over an extremely wide dose range.

BIRTH-DEATH MODEL: DISTRIBUTIONS OF TIME TO RESPONSE

In the preceding discussion of response probabilities, the only assumption made was that the organisms (or viral particles) act independently.

TABLE 4. *Effect of age on susceptibility of chick embryos to infection with Coccidioides immitis strain 6212*

Age of embryo (days)	Dose	Dead/eggs injected	Per cent mortality	LD_{50}	
				Reed and Muench	Weibull
5	180,000	10/10	100		
	18,000	10/10	100	794	800
	1,800	7/9	77		
	180	0/4	0		
6	180,000	10/10	100		
	18,000	9/9	100		
	1,800	7/10	70	676	800
	180	2/9	22		
7	180,000	8/8	100		
	18,000	5/9	55		
	1,800	3/10	30	7,762	6,000
	180	0/9	0		
8	180,000	9/9	100		20% hosts $d_1 \sim 1$
	18,000	5/8	62	5,495	80% hosts $d_2 \sim 10^4$
	1,800	2/10	20		
	180	2/10	20		
9	180,000	5/8	62		
	18,000	1/10	10	98,680	120,000
	1,800	0/10	0		
8	1,400,000	9/9	100		
	140,000	9/9	100		
	14,000	10/10	100		
	1,400	2/10	20		
	140	3/10	30		
	14	2/10	20		
	1.4	2/9	22		
	0.14	0/9	0		

From this assumption alone, we cannot obtain any information on the course of the infection, nor information on the time required to obtain an observable response. The term "response" will be used to denote the appearance of any of the various observed symptoms that are listed later in Table 7. By "time to response," we mean the time between challenge with an inoculum and first appearance of the symptom; that

is, time to response is equivalent to the variously used terms "incubation period," "latent period," "reaction time," "induction time," or "time to death."

To the assumption of independent action, we add now the simplest possible assumptions regarding the course of infection during the period before response—namely, that during this

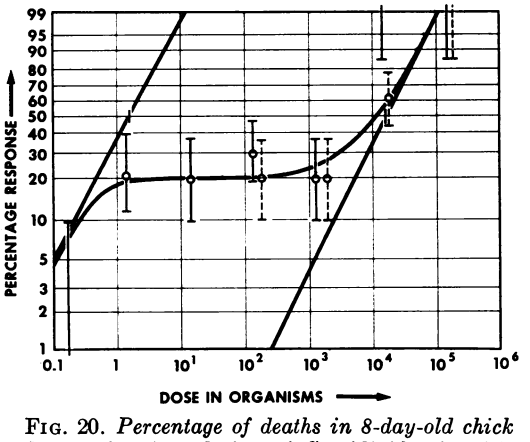

FIG. 20. *Percentage of deaths in 8-day-old chick embryos after inoculation of Coccidioides immitis by the yolk-sac route.*

TABLE 5. *Lethal response of guinea pigs inoculated intradermally with Pasteurella pestis encapsulated strain MP-6 in comparison with nonencapsulated mutant strain M-23*

Dose (organisms)	Deaths/total		Per cent mortality	
	MP-6	M-23	MP-6	M-23
9×10^8		10/10		100
9×10^7		10/10		100
9×10^6		8/10		80
9×10^5		10/10		100
9×10^4		5/10		50
9×10^3	10/10	3/10	100	30
9×10^2	10/10	5/10	100	50
9×10^1	10/10	2/10	100	20
9.0	10/10	1/10	100	10
0.9	2/10	0/10	20	0
0.09	0/10		0	

entire period the conditions that govern the probabilities of organism birth (cell division) and of organism death remain constant, independent of time and of number of organisms. During this period, as a result of chance, either all organisms will disappear or the total number of organisms will grow to a certain very large size, N, at which time response is assumed to occur, with the appearance of an observable symptom. The mathematical treatment of this so-called birth-death model in the papers by Saaty (50) and by Shortley (52) gives results that describe the distribution of response times

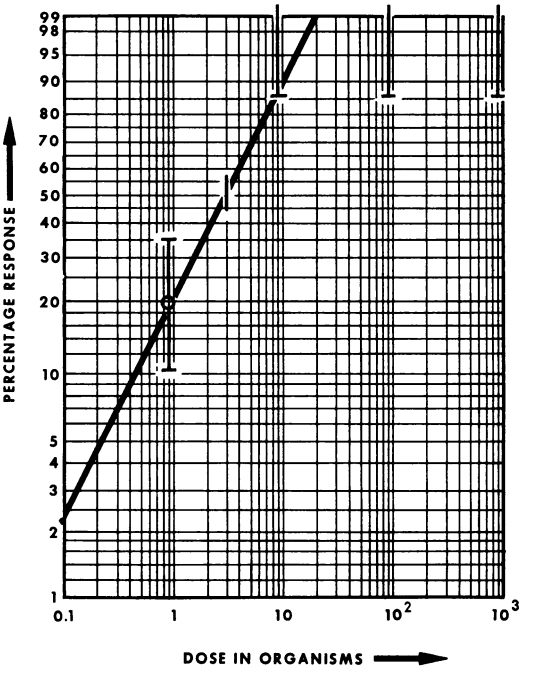

FIG. 21. *Percentage of deaths in guinea pigs after intradermal infection of Pasteurella pestis MP 6. (Compare with Fig. 22.)*

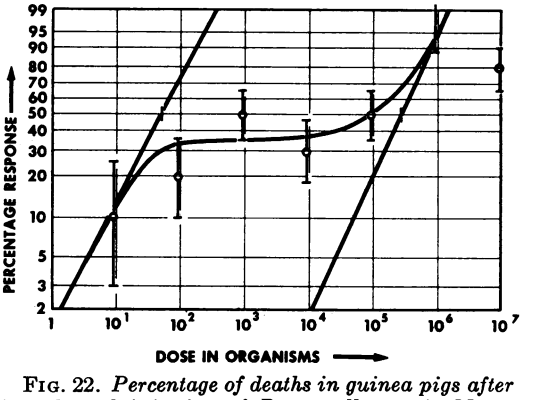

FIG. 22. *Percentage of deaths in guinea pigs after intradermal injection of Pasteurella pestis M 23. (Compare with Fig. 21.)*

and its dependence on challenge dose, and which are suitable for comparison with experimental data.

We shall first describe the structure of the birth-death model and shall then present the

results of the mathematical analysis in some detail. The model gives the same exponential response-probability function we have discussed in the preceding section. The model also gives results on time to response that are in qualitative agreement with the following experimental observations. Characteristically, the average time to response decreases as the dose increases, with an approximately linear relation between the average time and the logarithm of the dose. However, there is not a fixed time to response for a particular dose; rather, the times are distributed over a considerable range. This range is observed to be much wider for low doses that result in long average times than for high doses that result in short average times. Also, the distribution of times to response, for a given dose, is characteristically skewed and tails off toward the longer times.

TABLE 6. *Range of LD_{50} values in mice of various ages*

Age group	Range of LD_{50}*
7–23 hr	2×10–2×10^4
24–48 hr	1×10^2–1×10^5
3–5 days	1×10^3–1×10^6
6–7 days	2×10^4–2×10^7

* Expressed in pock-forming units.

Structure of the Model

The birth-death model in the simple form we shall describe in this section assumes that all organisms are identical (complete organism homogeneity), that all hosts are identical (complete host homogeneity), and that the mechanism of host-parasite interaction for each parasite in a host is identical—this means that all organisms initially locate at equivalent sites in a host. The last assumption of site homogeneity is, for example, not valid in respiratory infections where organisms can land on quite different types of tissue. The following section will give experimental evidence that organism-site heterogeneity, as well as the host heterogeneity already discussed, frequently exists.

In the birth-death model, during the period under consideration, the individual organisms in the inoculum act independently. Each organism in the original inoculum and in the resulting population of organisms in the host has a certain probability, denoted by λ, of dividing into two organisms per unit of time, and a certain probability, denoted by μ, of dying during this unit time interval. The probabilities λ and μ are considered as constants throughout the period prior to symptomatic response or organism disappearance, and are assumed to have the same value for each organism, host, and site. Although we realize that, for any one organism, these probabilities must fluctuate in time as the process of cell division goes on, we are working over a period involving many such divisions and involving a large number of organisms and, hence, we use a simple approximation in which these fluctuations are smoothed out and average values are employed.

The probability that any one organism will divide or die in a short interval of time can be interpreted as that proportion or fraction of the total population which can be expected to divide or die during that time. For example, if 1,000 bacteria are present in a host at a certain time and 12 of them can be expected to divide and 8 can be expected to die during the next minute, the value of λ is 12/1,000 = 0.012 per min and μ is 8/1,000 = 0.008 per min. We note that, if μ were zero, the mean time to division would be $1/\lambda$, which in the above example is 83 min. Similarly if λ were zero, the mean time to death would be $1/\mu$, which in the example is 125 min. If both λ and μ have values greater than zero, there is competition between the processes of birth and death; when λ is greater than μ, the mean time for a large colony to double in size (called the doubling time or generation time) is given by

$$\text{doubling time} = \frac{\log_e 2}{\lambda - \mu} = \frac{0.69}{\lambda - \mu} = \frac{0.69}{\alpha} \quad (12)$$

where we introduce α to denote the net probability of growth:

$$\alpha = \lambda - \mu \quad (13)$$

In our example, α = 0.004/min and the doubling time is 170 min. Defined in this way, α is the parameter that determines the exponential growth rate: for large colonies, the average colony size will increase in proportion to $e^{\alpha t}$.

In the birth-death model, the values of λ and μ alone determine the probability of response for any given challenge dose, but, to discuss time to response, we must introduce an additional assumption that determines a criterion for response. This assumption is that response occurs when the total number of organisms in the host reaches some definite large number which we designate by N. Thus, the period during which the probabilities λ and μ of birth and death have fixed values is assumed to be terminated either when the population of organisms in the host reaches zero and the infection dies out, or when the population reaches size N, and a symptom

appears. There is direct experimental evidence that response does occur at an approximately fixed number of organisms.

The birth-death model is said to be stochastic or probabilistic, because the postulated course of development of a disease has "chance" factors that make it impossible to predict the outcome of any one particular case. Thus, for a given dose of a given pathogen and a given host, the model cannot predict the exact value of response time, or even whether there will be a response. The model can, however, predict the percentage of hosts that will respond, predict the average time of response for those responding, and predict the distribution of times about the average, all as functions of the size of the challenge dose. By thus furnishing a "structure" for the analysis, the model can utilize data obtained from certain levels of challenge dose to predict the results to be expected from any arbitrary dose level.

The basic structure of the birth-death model is illustrated in Fig. 23. In this figure, which is highly schematic, the number of organisms in the colony in a host is represented on the vertical axis on a logarithmic scale, and time is represented on the horizontal axis on a linear scale. The letter d on the vertical axis represents the number of organisms in the initial challenge dose, and N is the number of organisms required for response. According to chance occurrences, the number of organisms will either increase from d to the large size N, and result in a response, or the number will decrease to zero and no response will result. The larger the number d in the initial dose, the greater will be the probability that the colony will increase to size N rather than decrease to size zero, and that a response will be the result.

Figure 23 shows the possible courses of events in six different hosts receiving the median infectious dose $d_0 = ID_{50}$, and also in six hosts receiving a much greater dose d. Since for the median infectious dose d_0 the probability of response is 50%, three hosts that receive this dose are assumed to respond, and three are assumed not to respond. For the much higher dose d, all six hosts are assumed to respond.

The wavy character of the lines in Fig. 23 suggests the elements of chance involved in the birth-death process. These elements of chance manifest themselves much more strongly when the number of organisms is small than when it is large. For a very large number of organisms, the growth is almost exactly exponential, as represented by a straight line on the semilog plot of Fig. 23. We can see from this behavior why the three growth patterns from the median dose d_0 are likely to result in widely different response times, while those growing from the much larger dose d will have response times differing only slightly.

The lines in Fig. 23 are purely illustrative and were not derived from the computations of the birth-death model or from experimental data; they are intended merely to illustrate schematically the behavior under the assumptions of the model. If a group of experimental animals is injected, each with the same dose d_0 or d of microorganisms under standard conditions, the growth pattern of the pathogens in any one animal is typified by one of the wavy lines in Fig. 23. If and when the threshold N is reached, a response

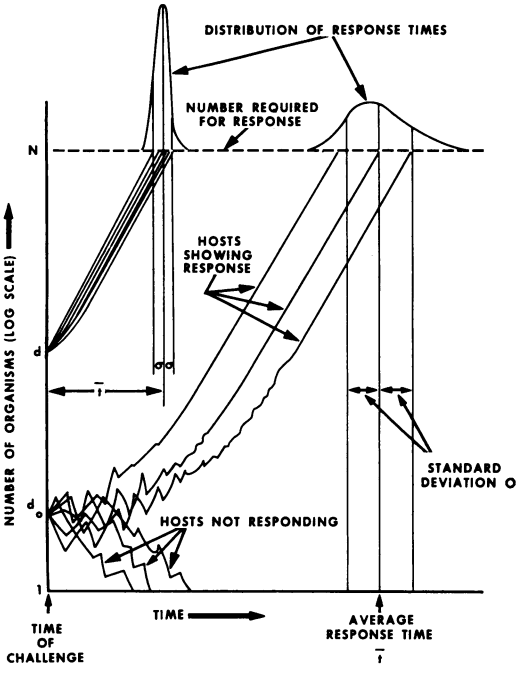

FIG. 23. *Course of birth and death (schematic).*

takes place. If a large group of animals is inoculated, one cannot predict which ones will respond nor at what time, but from test of such a group one can determine the proportion that respond, the mean or average response time $\bar{t}$, and the distribution of response times about this average. Such "frequency distributions" are shown by the curves drawn above the upper threshold line. A statistical measure of the "width" of these frequency distributions, called the standard deviation and denoted by σ, is also shown on these plots. A "positive skewness," or a tailing off toward longer times, that is predicted by the model is also indicated. This type of skewness is typically observed.

There is one assumption, not mentioned earlier, that is explicitly introduced in performing the mathematical analysis. This is the assumption that the challenge dose d is small compared with the number N of organisms required for response—say less than one-tenth of N. This assumption, which must be introduced to make the analysis tractable, amounts to saying that the model applies only when significant growth occurs during an "incubation" period before the response occurs. Thus, the model cannot be expected to apply to cases of "massive" doses near to or above the value N.

Predictions of the Model

Probability of response. Because in the birth-death model the organisms grow independently, and because the number N at which the organisms collectively cause infection is assumed large compared with the initial dose d, the probability of response is the same exponential function of d/d_0 (equation *1* and Fig. 2) that applies to an independent-action model. In addition, the model gives an explicit relation between the median infectious dose d_0 and the ratio μ/λ of death to birth probabilities. The relation is

$$d_0 = \frac{0.69}{1 - \mu/\lambda} \qquad (14)$$

The smallest possible value of μ/λ is zero. This value occurs when $\mu = 0$, a situation in which every organism grows and none dies. This situation, in which there is certainty of response whenever there is at least one organism in the inoculum, leads in *14* to the smallest possible median infectious dose, $d_0 = \log_e 2 = 0.69$ organism, as we have already discussed.

Values of μ/λ greater than zero correspond to higher values of d_0, with d_0 growing very large as μ/λ approaches 1. Equation *14* is only applicable when μ is less than λ; that is, when $\mu/\lambda < 1$. When the death probability μ is greater than the birth probability λ, the birth-death model gives zero probability of response—an inoculated colony always dies out and has no chance of growing to the large size N. In this discussion, we must remember the explicit assumption in the model that the challenge dose itself is small compared with N.

It is convenient to have equation *14* also in a form that gives μ/λ as a function of d_0. Algebraic manipulation of *14* gives the relation

$$\frac{\mu}{\lambda} = 1 - \frac{0.69}{d_0} \qquad (15)$$

Distributions of time to response. In Fig. 24 we give the curves, accurately computed from the model, that give the frequency distributions of time to response. These curves show the relative numbers of hosts responding in each unit of time for various challenge doses. The curves all have the same area, so they apply to hosts responding, not to hosts challenged. For example, of 100 hosts challenged with $d = 128\ d_0$, all 100 will usually respond (see Fig. 2 for response probabilities), with response times peaked as in the curve farthest to the left in Fig. 24. If 100 hosts are challenged with $d = 16\ d_0$, it is almost certain

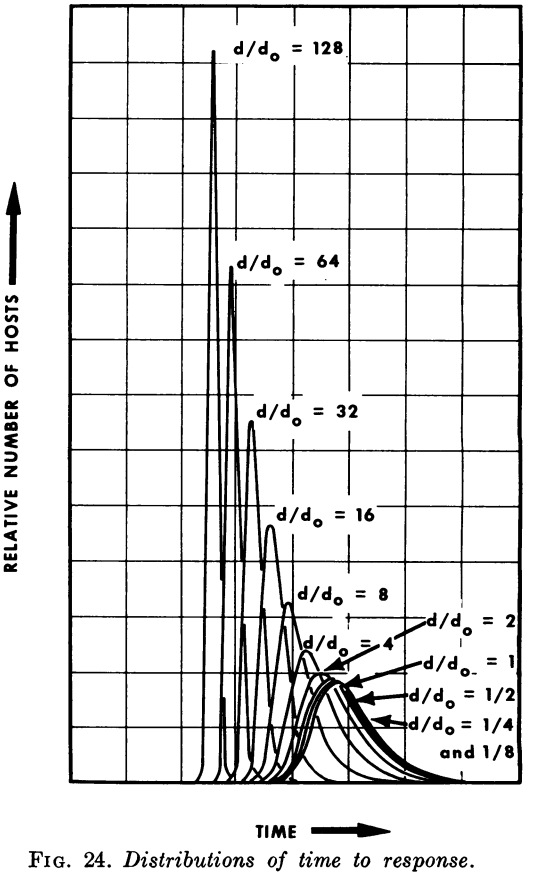

FIG. 24. *Distributions of time to response.*

that all 100 will respond, but the response times will be distributed according to the wider curve marked $d/d_0 = 16$. This curve is about one-third as high and three times as wide as the curve for $d/d_0 = 128$, indicating, roughly speaking, responses spread over about three times the time interval with, at the peak, only about one-third as many responding in a given time interval—say 1 hr. The curve for $d/d_0 = 1$ is even wider and lower but would still give the distribution of 100 animals responding. Now, however, since the response probability is only 50%, 200 hosts would

have to be challenged, on the average, to obtain the sample of 100 that respond. For even lower doses, still larger numbers would have to be challenged to obtain the sample that respond—it is to the responding sample that the curves apply.

Mathematical analysis demonstrates that the shapes of the curves in Fig. 24 are independent of the actual value of the median infectious dose d_0; they depend only on the ratio d/d_0. This feature is very convenient because it permits determination of these distribution curves by a single set of computations and their representation on a single chart. However, the size of the time unit on the plot is inversely proportional to

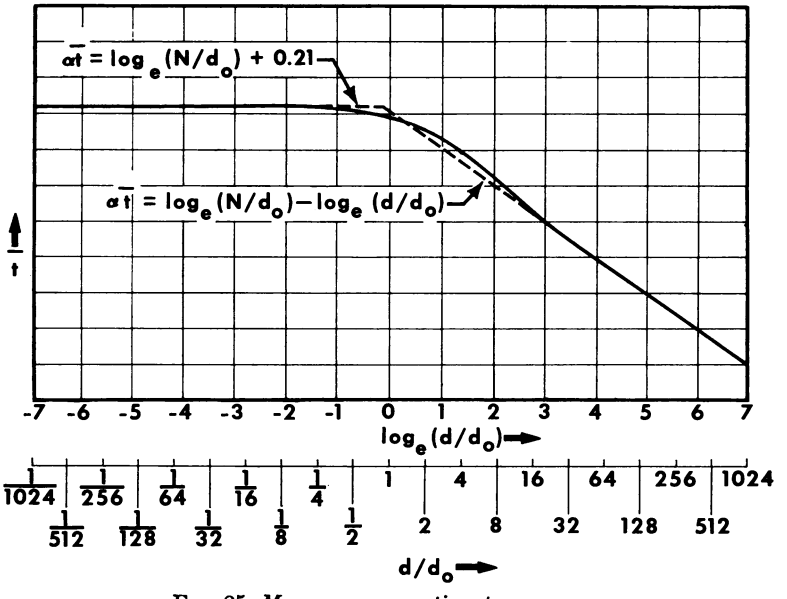

FIG. 25. *Mean or average time to response.*

$\alpha = \lambda - \mu$, which, according to equation *12*, determines the net rate at which growth takes place, whereas the placement of the curves relative to the time of challenge depends on the ratio N/d_0, which is related to the multiplication factor required before response occurs. For these reasons, the time unit and the time of challenge are not indicated in Fig. 24. Shortley (52) presented a detailed discussion of the appropriate time scales. For our biological comparisons, it will be simplest to describe these distributions in terms of the average time to response and the standard deviation of time to response that are indicated on Fig. 23. These quantities, as functions of d/d_0, are suitable for direct comparison with experimental data. Hence, we shall turn next to a description of these statistical parameters, as well as to the additional parameter related to skewness.

Before turning to this discussion, we note that the curves of Fig. 24 exhibit the various characteristics we have mentioned earlier. For doses above d_0, the average time decreases approximately linearly with the logarithm of the dose, moving in equal steps for each doubling of dose; the width (standard deviation) of the curves rapidly decreases with increasing dose; and there is a skewness with the longer tail to the right. We note that, on the contrary, for doses less than d_0 the curves rapidly approach coincidence so that for such low doses the distribution of time to response, the average time, and the standard deviation rapidly approach constant asymptotic values as the dose decreases.

Mean or average time to response. Figure 25 shows the behavior of the average time to response, $\bar{t}$, as a function of the ratio d/d_0. The average considered is the arithmetic mean. If a sample of hosts is tested at a given dose level, the average is computed by adding the response time of the hosts that do respond and dividing by the number of hosts that do respond.

It is shown in Fig. 25 that for doses less than d_0 the average time to response is predicted to be essentially constant. The reason for this constancy is that for doses substantially less than d_0 there is very little probability of infection at all; usually the progeny of all organisms die out. It turns out mathematically that with such low

doses, if the colony does succeed in growing to large size and causing infection, there is a very high probability that the large colony all represent the progeny of a single organism in the challenge dose; since the colony represents the progeny of a single organism, there is no variation in average time as the dose decreases—there is only a strongly decreasing probability of any infection at all.

In the region of doses above d_0, the curve rapidly assumes the form of a linear decrease of average time with increase in the logarithm of dose, according to the relation

$$\alpha\bar{t} = \log_e N - \log_e d = \log_e(N/d_0) - \log_e(d/d_0) \quad (16)$$

rabbits, with response time expressed as the number of days required for the development of a dark-field positive lesion. The value of d_0 is stated to be approximately two organisms. For d greater than 2, the observations fit a linear relation of the form of equation *16* with adequate accuracy. The bars in Fig. 26 show ±1 SE of the observed value of $\bar{t}$.

From Fig. 26, we can illustrate the method of computing the basic parameters λ, μ, and N of the birth-death process. We have seen that N represents the intercept of the straight line with the horizontal axis, which, on Fig. 26, is at $N \approx 5 \times 10^8$ organisms. This value gives the size to which the colony must grow before the lesion appears.

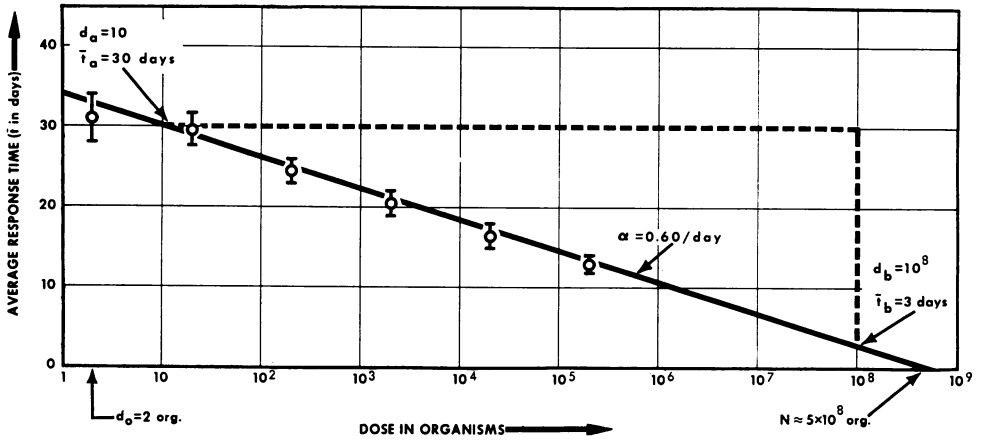

FIG. 26. *Typical linear regression of mean times to response for doses above d_0; the development of lesions by intracutaneous syphilis in rabbits.*

where $\alpha = \lambda - \mu$, as in equation *13*. The origin of time $\bar{t}$ is left indeterminate in Fig. 24, but must be chosen so that $\bar{t} = 0$ when $d/d_0 = N/d_0$, as indicated by equation *16*. In other words, the straight-line portion at the right of Fig. 25 crosses the axis of time at dose $d = N$.

By writing equation *16* in the form

$$\alpha\bar{t} = 2.30\,[\log_{10}N - \log_{10}d], \quad (17)$$

we see that, if $\bar{t}_a$ and $\bar{t}_b$ are the average times at doses d_a and d_b, α can be computed from the relation

$$\alpha = 2.30\,\frac{\log_{10} d_b - \log_{10} d_a}{\bar{t}_a - \bar{t}_b} \quad (18)$$

Figure 26 illustrates the behavior of the average time to response in the region of doses greater than d_0 in an experiment by Magnuson and Rosenau (37). The data are for intracutaneous inoculation of syphilis (*Spirochaete pallida*) in

The net growth rate $\alpha = \lambda - \mu$ can be obtained from the slope of the curve, as in equation *18*. If we take doses d_a and d_b 7 logs apart as indicated on Fig. 26, so that the numerator in equation *18* is 7, we have

$$\alpha = 2.30\,\frac{7}{(30-3)\text{ day}} = \frac{16.1}{27}\Big/\text{day} = 0.60/\text{day}$$

This value gives, according to equation *12*, doubling time = 1.2 days.

If we combine algebraically equations *13* and *14*, we find that λ is given in terms of α and d_0 by the relation

$$\lambda = \frac{d_0\,\alpha}{0.69} \quad (19)$$

In the case of Fig. 26, using $d_0 = 2$ and the value of α computed above, we find, from equation *19*, $\lambda = 1.74$/day. Correspondingly, we compute μ as $\mu = \lambda - \alpha = 1.14$/day.

We note that, whereas α is obtainable with considerable accuracy from the slope of the curve in Fig. 26, the value of λ (and hence of μ) contains, according to equation *19*, the same uncertainty as the value of d_0 which, in many cases like this one, is not known to a high degree of accuracy.

Finally, in comparing Fig. 26 with Fig. 25, we may ask for the predicted value of the constant mean response time for doses well below $d_0 = 2$ in Fig. 26. This value is given by the formula shown at the top of Fig. 25, which is applicable for doses that are small compared with d_0. This formula can be written as

$$\bar{t} = \frac{2.30 \log_{10}(N/d_0) + 0.21}{\alpha} \qquad (20)$$

where $d \ll d_0$. In the case of our example of Fig. 26, this relation gives

$$\bar{t} = \frac{2.30 \log_{10}(2.5 \times 10^8) + 0.21}{0.60/\text{day}} = 33 \text{ days}$$

as the constant average response time predicted for very low doses.

By following through these same arguments, with d_0 assumed to be known from data on response probabilities, the values of N, α, λ, μ, and the mean time to response for low doses can be obtained successively for any linear regression similar to that in Fig. 26.

Standard deviation and skewness. As we have stated previously, the standard deviation is a statistical measure of the width of the time distribution of response times. If the response times are expressed in days, the standard deviation can also be expressed in days and gives a standard measure of the spread of response time. As an example, for the dose 5×10^2 anthrax spores in Fig. 7, 30 hosts were challenged and 20 died. The histogram of Fig. 27 shows the distribution of days of death. As we shall compute in detail later, for this distribution, $\bar{t} = 2.4$ days and $\sigma = 1.4$ days, as indicated in Fig. 27.

As we have seen, the parameter α, which determines the net rate of growth, is appropriately measured in day^{-1}. The product $\alpha\sigma$ is, thus, dimensionless. For the birth-death model, the parameter $\alpha\sigma$ is determined purely by the ratio d/d_0, and has the values given in Fig. 28. The values of $\alpha\sigma$, and hence of σ itself, are predicted to be essentially constant for doses less than d_0 and to decrease rapidly for doses higher than d_0. This decrease is systematically observed. For example, for the anthrax data of Fig. 7, σ decreases from 1.4 days at the dose 5×10^2 organisms to about 0.1 day at the largest doses.

The skewness is a statistical measure of the asymmetry of a distribution such as that in Fig. 27. In Fig. 27, the number of mice dying per day clearly falls off less rapidly as we move to the right of the day of maximal deaths than it does as we move to the left. The distribution is said to have its longer tail to the right, and statistically this corresponds to a positive value of the skewness. A symmetrical curve would have

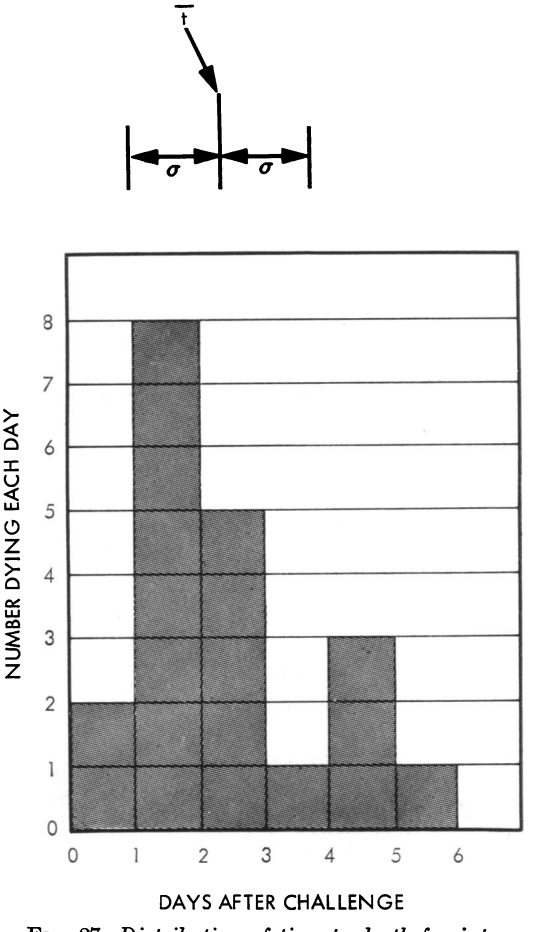

FIG. 27. *Distribution of time to death for intraperitoneal injection of 500 anthrax spores in mice.*

zero skewness; one tailing off to the left would have negative skewness.

Distributions of times to response are characteristically observed to have positive skewness. Skewness is a dimensionless quantity. The birth-death model predicts that its value depends purely on d/d_0, with the dependence indicated by the second curve in Fig. 28.

Table 7 shows the details of the computation of estimates of $\bar{t}$, σ, and skewness for the data in the sample of Fig. 27. Let us compare the values

predicted on Fig. 28 with those computed in Table 6 for this example.

At the dose of 5×10^2 organisms in Fig. 7, essentially all of the hosts responding will be of the sensitive type having median lethal dose $d_0 = d_1 = 25$ organisms. Hence, for this dose, $d/d_0 = 500/25 = 20$. For this ratio, Fig. 28 predicts that $\alpha\sigma$ will be about 0.4 and the skewness about 0.9. The observed skewness, 0.93, is very close to the predicted value. Such agreement of skewness is frequently found. To compute $\alpha\sigma$, we need to obtain a value of α from a plot similar to that of Fig. 26. Such a plot gives a value of α of approximately 6/day and hence an observed value of $\alpha\sigma \sim 8$. This value is many times greater than the value of 0.4 predicted by the model. Observed values of $\alpha\sigma$ are always found to be greater than those predicted. Even if the model parameters λ, μ, and the exponential growth rate $\alpha = \lambda - \mu$. That discussion assumed complete homogeneity.

Host homogeneity is required for the simple birth-death model to apply. A Weibull response plot shows the data of Fig. 26 to meet this host-homogeneity criterion: 90% of the hosts are sensitive, with d_0 of the order of two organisms; the other 10% are so resistant that almost none responds for doses in the range plotted in Fig. 26, so we have an essentially homogeneous host group.

It is also necessary that the organisms be homogeneous—and arrive at sites in the host that are equivalent from the standpoint of factors affecting organism growth and death. If, for example, because of differences in virulence or of host site, only 10% of the organisms are capable

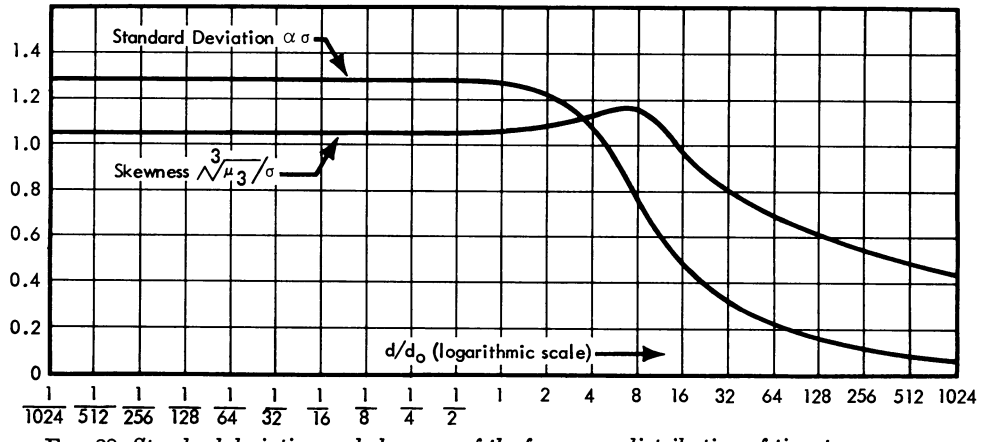

FIG. 28. *Standard deviation and skewness of the frequency distribution of time to response.*

is basically sound, greater standard deviations would be expected in practice because of the fact that the model assumes perfect homogeneity. All sources of heterogeneity, which undoubtedly exist, would be expected to widen, rather than to narrow, the frequency distribution curve. Heterogeneity in hosts, organisms, or organism location in the host would lead to distributions of values, not fixed values as assumed, of the basic parameters λ, μ, α, and N, and it is readily seen that such distributions of values can drastically spread out the times to response.

BIRTH-DEATH MODEL: COMPARISONS WITH EXPERIMENT

We have seen, in the preceding pages, how the linear relation between average response time and log dose can be used, together with the value of median infectious dose d_0, to obtain the of growth after inoculation, then the value of α given by equation *18* will be accurate for this 10% of the organisms, but the value of λ given by equation *19* will come out too high by a factor of 10, as will the value of N.

Host heterogeneity is readily detected by the methods described above in the section on the independent-action model. Organism or site heterogeneity is less readily detected, but is, as we shall discuss presently, undoubtedly responsible for the large values of d_0 frequently observed, and possibly for the initial decrease in number of organisms that is also frequently observed in direct counts. For this reason, we can have no confidence in the value of λ computed from equation *19*, nor in the corresponding value of μ.

Table 8 summarizes the data that we have found in which mean response time has been determined as a function of challenge dose, and which are adequate to determine a value of α

(the exponential growth rate) from the slope of a curve such as that in Fig. 26. This table includes 14 of the 16 cases listed by Meynell and Meynell (40) as observed to give a linear relation between $\bar{t}$ and log dose, as well as a considerable number of additional cases. The table lists d_0, α, and N (α and N/d_0 in the case of viruses), but does not list computed values of λ and μ because of uncertainties as to the interpretation of these parameters, as discussed in detail below.

It is interesting to note in Table 8 that the values of α are characteristically of the order of magnitude of 1/day, which corresponds to a doubling time of 0.69 day or 17 hr. The largest growth rate in the table is about 17/day, which occurs for pneumococci injected intraperitoneally day. By actual count, the shortest observed organism doubling times are of the order of magnitude of 1 hr, corresponding to a value of α of 17/day, the fastest rate occurring in Table 8. Values of λ significantly larger than 17/day would not be expected to occur.

A case in point, although not an extreme case, is illustrated in Fig. 29. This figure shows another set of data by Magnuson and his colleagues (38) on intracutaneous syphilis in rabbits. Although the *Treponema pallidum* is of the same strain as that used in Fig. 26, where d_0 was 2 organisms, a Weibull plot of response percentages shows that the value of 23 organisms given for the present trials is acceptable, with some 5% of the hosts having an even higher d_0.

TABLE 7. *Computation of estimates of mean time to response, standard deviation, and skewness, for the data of Fig. 27*

t (days)	n_t	$n_t t$	$t - \bar{t}$	$(t - \bar{t})^2$	$n_t(t - \bar{t})^2$	$(t - \bar{t})^3$	$n_t(t - \bar{t})^3$
0.5	2	1.0	− 1.9	3.61	7.22	− 6.86	− 13.72
1.5	8	12.0	− 0.9	0.81	6.48	− 0.73	− 5.84
2.5	5	12.5	+ 0.1	0.01	0.05	+ 0.00	0.00
3.5	1	3.5	1.1	1.21	1.21	+ 1.33	+ 1.33
4.5	3	13.5	2.1	4.41	13.23	+ 9.26	+ 27.78
5.5	1	5.5	3.1	9.61	9.61	+ 29.79	+ 29.79

$n = \Sigma n_t = 20$

$\Sigma n_t t = 48.0\ d$

$\bar{t} = \dfrac{\Sigma n_t t}{n} = 2.4\ d$

$\Sigma n_t(t - \bar{t})^2 = 37.80$

$\sigma^2 = \dfrac{\Sigma n_t(t - \bar{t})^2}{n - 1}$

$= \dfrac{37.80}{19} = 1.99\ d^2$

$\sigma = \sqrt{1.99} = 1.4\ d$

$\Sigma n_t(t - \bar{t})^3 = 39.34$

$\mu_3 = \dfrac{n}{(n-1)(n-2)} \Sigma n_t(t - \bar{t})^3$

$= \dfrac{20}{19 \cdot 18} \times 39.34$

$= 2.30\ d^3$

Skewness $= \sqrt[3]{\mu_3}/\sigma = \sqrt[3]{2.30}/1.4 = 0.93$

Standard error of $\bar{t} = \sigma/\sqrt{n} = 1.4/\sqrt{20} = 0.3\ d$

in mice; this value corresponds to a doubling time of 1 hr, and is of the same order of magnitude as the shortest doubling times observed by direct counts in vitro or in vivo. The smallest value of α in the table is for the very slow-growing bacillus of human leprosy injected in the foot pads of mice; this value is 0.8/month or 0.027/day and corresponds to a doubling time of 0.9 month.

Effects of Organism or Site Heterogeneity

There are many instances in the literature in which very large values of median infectious dose d_0 occur, but in which the exponential growth rate α has its characteristic value of the order of 1/day. In these cases, equation *19*, $\lambda = d_0\alpha/0.69$, gives a value of λ that is untenably large from the biological point of view—a value that may be in the hundreds, thousands, or even millions per

From the value $d_0 = 23$ organisms and the value $\alpha = 0.63$/day given by Fig. 29, we find $\lambda = 21.0$/day and $\mu = \lambda - \alpha = 20.4$/day. Even for this nonextreme instance, these values ($\lambda = 21.0$/day, $\mu = 20.4$/day) are unacceptable. A biological system cannot operate like clockwork, with the small difference between large values of λ and μ representing the exact net growth rate. The computed values of λ and μ must always represent some sort of averages over distributions of values, with organisms, organism environments, and time as variables. But even a slight smearing out of the above "average" values will give some situations in which $\mu > \lambda$. We remember that in this case, where μ is greater than λ, the model gives no probability of the inoculum growing to large size and, in fact, the organisms will all die.

TABLE 8. *Parameters of the birth-death model*

Type of organisms	Disease	Host	Route	Symptom	d_0 (organisms)	α (day^{-1})	N^* (organisms)	Comments	Reference†
Bacteria	Syphilis	Rabbits	Intracutaneous	Visible lesion	2	0.60	5×10^8	Some host heterogeneity. $d_0 \sim 2$(75%), $d_0 \sim 100$(15%), $d_0 \sim 10^5$(10%). Excellent linearity of $\bar{t}$ vs. log d (see Fig. 26).	(36, 37)
	Syphilis	Rabbits	Intratesticular	Palpable lesion	1	0.56	2×10^7	$\bar{t}$ approximately constant out to $d = 10^3$, then decreases linearly. Authors suggest possible "migration."	(36)
	Syphilis	Rabbits	Intracutaneous	Visible lesion	23	0.63	2×10^8	See Fig. 28 and 29.	(38)
	Syphilis	Humans	Intracutaneous	Visible lesion	~57	~0.7	$\sim 10^9$	Only four doses, eight subjects each.	(38)
	Tularemia	Mice	Subcutaneous	Death	0.7–3.6	2.8–5.6	$\sim 10^{13}$	Data given for 10 organism strains and 8 doses from about 10 to 10^8 organisms; excellent linearity for all strains.	(4)
	Tularemia (Schu)	Guinea pigs	Subcutaneous	Death	1.6	4.1	$\sim 10^{15}$	Doses 10^2–10^9 organisms; fair linearity of $\bar{t}$ vs. log d.	(4)
	Tularemia (425 $F_{30}G$)	Guinea pigs	Subcutaneous	Death	9.4	1.7	$\sim 10^{12}$	Doses 10^2–10^9 organisms; fair linearity of $\bar{t}$ vs. log d.	(4)
	Tularemia (Schu)	Mice	Intraperitoneal	Death	0.76	4.2		Growth at rate of 4.2/day up to 10^7 organisms; then a faster growth rate (see Fig. 36). Other strains show different behavior (see Fig. 37) and some high values of d_0.	(a)
	Anthrax	Mice	Intraperitoneal	Death	See Fig. 7	~6	$\sim 10^{12}$	Growth rate quoted is for doses less than 10^6; growth rate doubles for higher doses.	(b)
	Anthrax	Mice	Subcutaneous	Death		5.5	$\sim 10^9$	Good linearity of $\bar{t}$ vs. log d.	(8)
	Anthrax	Rats	Intraperitoneal	Death		6	$\sim 10^{13}$	Data available only for doses greater than 10^5.	(b)
	Anthrax	Hamsters	Intraperitoneal	Death	<10	~5	$\sim 10^{12}$	Growth rate quoted is for doses less than 10^5; $\alpha \sim 11$ for higher doses.	(b)
	Pneumococcus	Mice	Intraperitoneal	Death		17	$\sim 10^{14}$	For animals treated with sulfapyridine, the value of α was decreased to 6.2/day, with no significant change in N.	(13)
	Leptospirosis (*L. icterohaemorrhagiae*)	Guinea pigs	Intraperitoneal	Death	2, 10, 100 (3 strains)	2.6 2.0	10^{12}‡ 10^8–10^9	From curve of time to death. From direct counts.	(20)
	Human tuberculosis	Mice	Intravenous	Death		~0.15	8 mg	Immediate death with 10 and 12 mg.	(57)
	Human tuberculosis	Mice	Subcutaneous	Death		~.46	$\sim 10^{15}$		(46)
	Human tuberculosis	Guinea pigs	Intraperitoneal	Death	<100	~0.05	$\sim 10^8$		(6)
	Human leprosy	Mice	Injection in footpad	Microscopic lesion		~0.8/month	$\sim 10^6$	Harvest of organisms in lesion gave $N \sim 10^6$ and a doubling time, compared with the initial inoculum, of ~0.9/month, corresponding to $\alpha = 0.8$/month. A roughly linear relation between incubation period and size of inoculum gives N and α of the same orders of magnitude.	(51)

	Plague	Guinea pigs	Inhalation	Death		4.2		From direct counts. An initial drop in count by a factor of about 100 is observed. See Fig. 30.	(23)
	Plague	Guinea pigs	Intratracheal	Death	~5	~1.9	~3×10^6		(c)
	Plague	Mice	Intraperitoneal	Death	~5	~2.0	~10^6		(c)
	Plague	Guinea pigs	Intradermal	Death	~1	~1.1	~3×10^6		(c)
	Mouse typhoid	Mice	Intraperitoneal	Death	See Fig. 9	See Fig. 31	10^8–10^9		(40)
	Mouse typhoid	Mice	Intraperitoneal	Death	~2	2.2	10^9–10^{10}	Swiss mice—very homogeneous hosts.	(45)
	Mouse typhoid	Mice	Intraperitoneal	Death		1.0	10^8–10^9	Time to death measured and direct counts made. See Fig. 39.	(5)
Viruses	Smallpox	Mice <24 hr old	Intracerebral	Death		~2.9	~10^{12}	Data for only four dosage values, all low doses. Hosts fairly homogeneous.	(39)
	Smallpox	Suckling mice	Intraperitoneal	Death		~1.2	~10^4	N and d_0 both increase regularly with age. See Fig. 12 for response percentages.	(39)
	Leukosis (avian erythromyeloblastic leukosis virus)	Chickens	Intravenous	Primitive cells in blood		~1		An extraordinarily flat dose-response probability curve, requiring dose increase by 6 logs to go from 20 to 80%—possibly indicating very heterogeneous hosts; possibly unexplained.	(18)
	Mouse-pox	Mice (footpad)	Subcutaneous	Swelling		2.7	~10^{12}	Two strains of ectromelia virus.	(22)
	Encephalomyelitis (strain GD VII)	Mice	Intracerebral	Sickness		1.0	~10^8	Excellent linearity of $\bar{t}$ vs. log d.	(24)
	Poliomyelitis	Mice	Intracerebral, intraperitoneal	Paralysis		~4	~10^{10}		(30)
	Poliomyelitis	Rhesus monkeys	Intracerebral	Paralysis		~3	~10^{13}	Five strains show similar results.	(7)
	Rift Valley fever	Mice	Intracerebral	Death		11	~10^{12}		(41)
	Measles	Human children	Subcutaneous	Fever		0.9		Tests on 10 children with doses varying over 5 logs show good linearity of $\bar{t}$ vs. log d.	(d)
	Meningopneumonitis	Chick embryos	Yolk sac	Death		3.8	10^8–10^{10}	Excellent linearity of $\bar{t}$ vs. log d. Homogeneous hosts.	(14, 15)
	Feline pneumonitis	Chick embryos	Yolk sac	Death		1.8–4.2	~10^8	Three strains of organisms gave α values 1.8, 3.5, and 4.2/day. There was a good linearity of $\bar{t}$ vs. log d for all three strains.	(56)
	Murine pneumonitis	Mice	Respiratory	Death		0.50		This value of α applies for a certain dose range; for higher doses α is greater.	(25)
	Bronchopneumonia virus	Mice	Intranasal	Death		0.9			(27)
	Psittacosis	Chick embryos	Yolk sac	Death		3.9	~10^{10}	Excellent linearity of $\bar{t}$ vs. log d. Homogeneous hosts.	(26)
	Papilloma virus	Rabbits	Skin scarification	Wart		0.55	~10^6	Excellent exponential dose response with 5% inhomogeneity. Excellent linearity of $\bar{t}$ vs. log d, but $\bar{t}$ continues to rise for doses below d_0, significantly at 5% level. See Fig. 33 and 34.	(10, 11)

TABLE 8—*Cont.*

Type of organisms	Disease	Host	Route	Symptom	d_0 (organisms)	α (day^{-1})	N^* (organisms)	Comments	Reference*†
	Rous Sarcoma virus	Chicken wing web	Subcutaneous	Tumor, detectable by sight through translucent web		1.5	$\sim 10^7$	Two experiments: (1) homogeneous chickens, good exponential response probability; (2) "heterogeneous" chickens, 95% having the same d_0 as the homogeneous, 5% having d_0 higher by 10^3. Good linearity of $\bar{t}$ vs. log d.	(9)
	Adenoviruses	Hela tissue culture	Inoculation	Cytopathogenic effect		1.3–2.0	$\sim 10^8$	Good linearity between $\bar{t}$ and log d.	(31)
Rickettsia	Scrub typhus	Men	Intradermal	Primary lesion		0.9	$\sim 10^4 d_0$		(34)
				Fever		0.9	$\sim 10^6 d_0$		
	Q fever	Men	Respiratory	Fever	~ 1	1.2	10^8–10^9		(55)
	Q fever	Guinea pigs	Respiratory	Fever	~ 1	1.6	10^8–10^9		(55)
	Q fever	Guinea pigs	Intraperitoneal	Fever	~ 1	2.3	10^8–10^9		(55)
	Q fever	Guinea pigs	Intraperitoneal	Fever		1.6	$\sim 10 d_0$		(e)
	Q fever	Chick embryos	Yolk sac	Death		0.9	$\sim 10^{10}$		(43)
Protoza and tumor cells	Toxoplasmosis (*T. gondii* in human serum)	Mice	Intraperitoneal	Death	<1	3.4	$\sim 10^{13}$	Good linearity of $\bar{t}$ vs. log d; good host homogeneity.	(19)
	Toxoplasmosis (*T. gondii* in saline)	Mice	Intraperitoneal	Death	30	1.8	$\sim 10^{10}$	Good linearity of $\bar{t}$ vs. log d; 10% host heterogeneity.	(19)
	Trypanosomiasis	Rats	Intraperitoneal	Death		~ 0.7	$\sim 10^9$	For 35–40 g rats	(32)
							$\sim 10^{12}$	For 50–55 g rats	
	Adenocarcinoma	Mice	Subcutaneous	Palpable tumor	2,000	0.38	2×10^6	Marsh-Simpson tumor. Size at palpability, 0.5 mm^3; exponential growth shown to continue up to 100 mm^3. Good exponential dose-response probability curve.	(28, 48)
	Ehrlich ascites tumor	Mice	Intracerebral	Death	~ 16	0.69		Average of 17 trials. Good exponential dose response.	(47)

* For viruses, N/d_0.

† Numbers indicate references in Literature Cited. Letters represent unpublished data as follows: (a) U. S. Army, (b) R. E. Lincoln, (c) M. J. Surgalla, (d) F. McCrumb, (e) V. W. Andrew and J. C. Wagner.

‡ In these experiments, direct counts after inoculation of large doses show an initial drop in numbers of organisms by a factor of 100 or more; this drop may account for the differences in N.

We can give a much more satisfactory explanation of the value $d_0 \sim 20$ organisms for these trials, in comparison with the value $d_0 \sim 2$ organisms in Fig. 26, by assuming that, in the particular inoculum used in these trials, only about 10% of the organisms have $\lambda > \mu$ and are capable of growing to colonies of large size, while 90% of

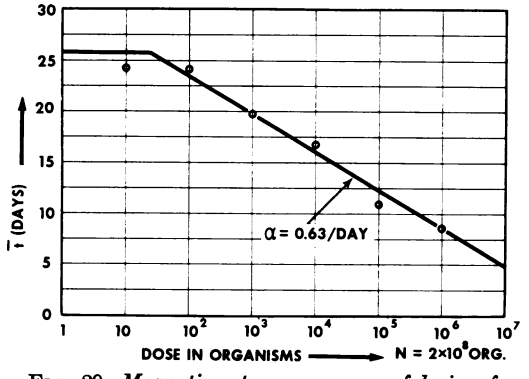

FIG. 29. *Mean time to appearance of lesion for intracutaneous syphilis in rabbits ($N \approx 2 \times 10^8$ organisms).*

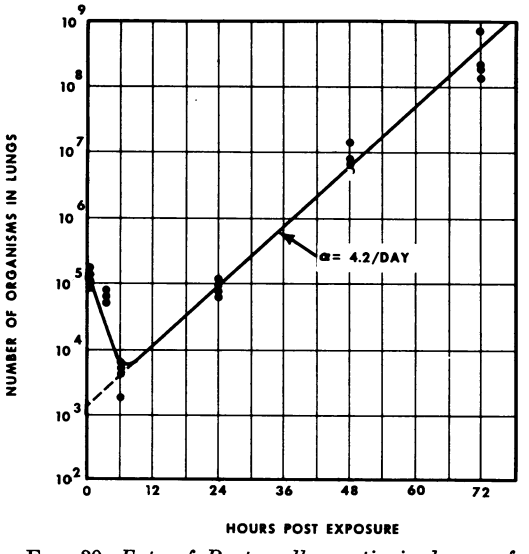

FIG. 30. *Fate of Pasteurella pestis in lungs of aerosol-exposed guinea pigs.*

the organisms die out. We are then back to exactly the situation of Fig. 26 and obtain more reasonable values of λ and μ, of the order of magnitude of those given previously.

There is strong biological evidence that an initial shrinkage in colony size (by a factor of 10 to 100 or more) does frequently occur before the regular growth pattern sets in. For example, Fig. 30 shows lung counts of guinea pigs immediately after inhalation of *Pasteurella pestis* strain Alexander, and at subsequent times thereafter (23). There is a drop in count for 6 hr and then a regular exponential growth until death, at a growth rate corresponding to $\alpha = 4.2$/day. The drop lowers the effective dose at time zero by a factor of 100. This drop is accompanied by a greatly increased rate of phagocytosis by lung macrophages. The bacteria cleared from the lungs were demonstrated not to have migrated to other parts of the guinea pig.

In other, unpublished work from the same laboratory where the results in Fig. 30 were obtained, the median lethal dose for respiratory infection of guinea pigs with this organism was found to be of the order of $d_0 = 4{,}000$ cells. Any attempt to compute values of λ and μ using the above values of α and d_0 would give absurdly large rates. However, the effective d_0 must be reduced by (i) the fraction of organisms inhaled that do not lodge in suitable sites in the lungs and (ii) the fraction lodged in the lungs that are destroyed by phagocytosis, or other defense mechanisms, in the early period after challenge.

Many other data of the type shown in Fig. 30, indicating a strong initial decrease in colony size, are to be found in the biological literature, both for bacteria (5, 20) and for viruses (1, 39).

We conclude from our literature survey that there are few systems for which meaningful values of λ and μ can be obtained. In fact, the only clear-cut cases are those in which d_0 is found to be 0.69 organisms, in which case we are sure that $\lambda = \alpha$ and $\mu = 0$.

Constancy of Mean Time to Response at Low Doses

Experiments on Salmonella typhimurium. We have found just one set of experiments, by Meynell and Meynell (40), designed specifically to check the constancy of the mean response time (time to death in this case) for doses below the median infectious dose. Unfortunately, in these experiments, there is strong host heterogeneity that masks the effect being sought. We cannot agree with the authors that these experiments demonstrate approximate constancy of mean response time at doses below the LD_{50}.

Figure 31 shows the response percentages for experiment 1 of this set of experiments on the intraperitoneal injection of mice by *S. typhimurium*, the response being death. For these data, Meynell and Meynell give $d_0 = 320$ organisms. However, it is clear from Fig. 31 that the hosts fall into two groups. Approximately 44% of the hosts are susceptible, with d_1 very small. Lack of data at doses lower than 5.1 organisms precludes fixing the left-hand asymptote, but the smallest possible d_1 is 0.69 organisms; curves are

drawn both for $d_1 = 0.69$ and $d_1 = 3$; the true value of d_1 would seem to lie between these limits. The position of the upper asymptote gives a value of d_2, for the resistant hosts, in the neighborhood of 6,000 organisms.

For doses below about 600 organisms (0.1 d_2), substantially all of the observed responses will result from the susceptible group of hosts. The

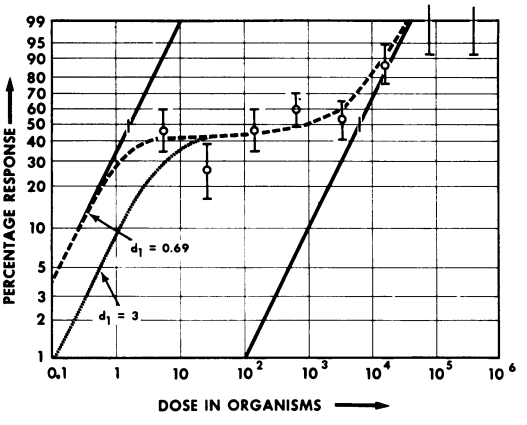

FIG. 31. *Percentage of deaths in mice infected intraperitoneally with Salmonella typhimurium. Experiment 1 of Meynell and Meynell (40).*

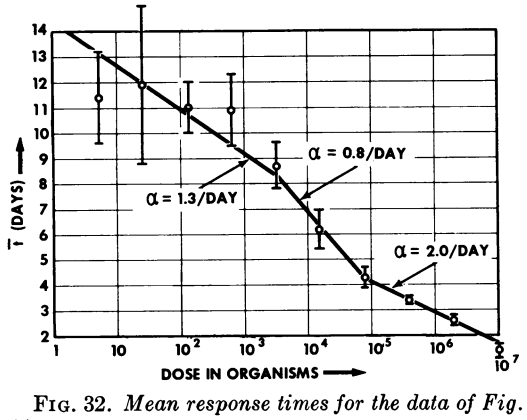

FIG. 32. *Mean response times for the data of Fig. 31.*

observed mean times to response, with ±1 SE indicated, are shown in Fig. 32. Since there is only 68% probability that the true mean is within ±1 SE of the observed mean, the data for the first four points of Fig. 32 are not inconsistent with the indicated straight line, of some such slope as would be expected. There is indication of change of slope of this line when we enter the regime of resistant hosts, at about 6,000 organisms, and another change in slope, corresponding to an increase in growth rate, at about 10^5 organisms.

The experiment described above had other interesting features. Terminal viable counts were made, shortly after death, on mice inoculated at each dosage level indicated in Fig. 31 and 32; all terminal counts were approximately constant in the range from about 10^8 to 10^9 organisms, regardless of size of challenge dose. This is also the range in which the straight line at the right of Fig. 32 would cross the axis $\bar{t} = 0$. Counts were also made on sacrificed mice at various times after inoculation. In mice challenged with 8×10^4 and 2×10^6 organisms (in the 100% response region in Fig. 31, the colony growth patterns were entirely consistent with the rate of growth given by $\alpha = 2.0$/day at the right of Fig. 32. In mice challenged with 3×10^3 organisms, the general growth rate seemed to be slower, and the mice seemed to divide into two groups, those that would presumably have died and those that would have survived. However the colony sizes in the latter group seemed to increase for a few days and then to decrease—a behavior inconsistent with a model in which conditions are independent of time or colony size.

Meynell and Meynell (40) also give data for their experiments 2 and 3, which were replicates with combined response percentages which have already been shown in the three-group curve of Fig. 9. Their data on average response times are again so badly scattered that their conclusion that this time tends to constancy for doses less than their LD_{50} of 3.2×10^6 organisms seems not to be well supported.

Experiments on papilloma virus. The section on the independent-action model contained examples showing that viruses, as well as bacteria, can give response-probability curves that are described by simple exponentials and, hence, conform to the independent-action model.

The data on times to response for viral infections that are listed in Table 8 conform to the predictions of the birth-death model about as well as do the data for bacteria. Linear relations between $\bar{t}$ and $\log d$ are characteristically observed; the distribution of times is skewed to the right; and standard deviations decrease with increasing dose but are characteristically larger than those predicted.

Figure 33 shows the average time for development of rabbit warts after challenge with various quantities of papilloma virus by means of skin scarification (10). The value of d_0 given on this figure was determined from a separate set of experiments (11) that led to response percentages that indicate the hosts are 95% homogeneous.

The two sets of experiments are believed by the authors to represent comparable data, because purified papilloma virus protein was used and identical experimental techniques were employed. If the data are indeed comparable, then, with statistical significance, the points on Fig. 33 for doses less than d_0 fail to approach a constant mean response time, as is predicted by the birth-death model.

Other explanations of the above discrepancy are possible, and this isolated example is not to be regarded as a conclusive test. However, there is serious question as to whether the basic assumptions of the birth-death model would be expected to apply to viruses, because the process of replication of viruses is considerably more complex and inherently different from the process of binary fission of bacteria. A detailed model for the behavior of viral particles should be based on an assumption different from that of binary fission, which was used to obtain the mathematical results described in the action on the birth-death model. Changes in the detailed assumptions regarding the mechanism of replication would be expected to result in significant changes in the predictions of a mathematical model in the region of low doses and in little change in the character of the predictions for doses well above d_0.

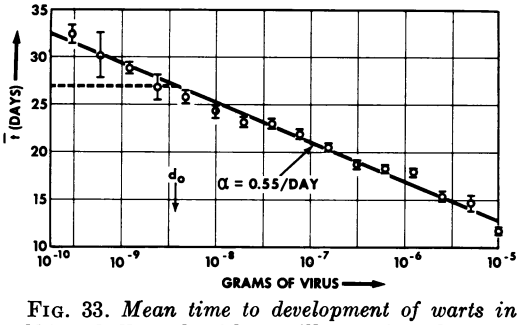

FIG. 33. *Mean time to development of warts in rabbits challenged with papilloma virus by skin scarification.*

Variation of Growth Rate with Colony Size

If the slope α of the curve in the plots of $\bar{t}$ versus $\log d$ is interpreted as the exponential growth parameter, as evidence seems to justify, then, in cases where the observed response is death, it is frequently observed that the growth parameter changes with the number of organisms. An example in which α seems definitely to increase when the inoculum gets to within a factor of 10^4 of that at death has already been exhibited in Fig. 32. A similar increase is shown in the U.S. Army data on tularemia given in Fig. 34. As noted in Table 8, a similar phenomenon occurs for anthrax in mice and hamsters.

The reverse behavior is sometimes observed, with an apparently slower growth rate at large numbers of organisms; Fig. 35 shows an example from U.S. Army data. This figure applies to a different strain of *P. tularensis* than that used in Fig. 34. Four trials were run, and there was an apparent change in virulence after trial II such that the d_0 increased from its minimal possible value of 0.69 organism for trials I and II to 1,700 and 1,400 organisms for trials III and IV, respectively. Trials I and II show an approximately constant rate of growth at α about 4.5/day out to an N of about 10^{10}. Trials III and IV show distinctly longer times to death, but about the same growth rate as trials I and II out to doses of about 10^8, and then an apparently slower growth rate at α about 1.3/day to a value of N approximately the same as that in trials I and II.

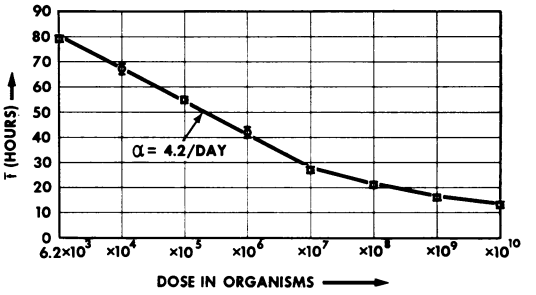

FIG. 34. *Mean time to death of mice infected intraperitoneally with Pasteurella turlarensis Schu (d_0 = 0.76 organism).*

There is evidence of similar behavior in the work of Marshall and Gerone (39) on variola virus in suckling mice. Their direct counts, in terms of pock-forming units, after the initial decrease in virus, show rapid growth for 3 or 4 days, then an essentially constant count for 3 or 4 days until death.

Distributions of Time to Response

Figure 36 shows a plot of unpublished data taken by V. W. Andrew and J. C. Wagner on day of death of guinea pigs inoculated intraperitoneally with whole-egg suspensions of the rickettsia *Coxiella burnetii*, the causative agent of Q fever. The plot shows, for various dose levels, the number of hosts responding on each day, given as a percentage of all the hosts that respond. The superposed hatched curves give the percentage response each day computed from the birth-death model, using the values of α and

N/d_0 obtained from plots similar to those we have discussed, entered in tables given by Shortley (52). A Weibull plot of the response percentages shows the hosts to be 95% homogeneous with the value of d_0 given by the experimenters, the balance of the hosts being completely resistant to the dose range in question. The relation between $\bar{t}$ and $\log d$ is excellently linear.

The predicted distributions of time to death for the three highest doses in Fig. 36 are very narrow, with σ values of 0.1 day or less according to Fig. 28. Hence, the hatched curves are plotted to show all of the deaths occurring on the same day. For $d/d_0 = 15$, the predicted deaths are spread over 2 days, and for $d/d_0 = 1.5$, they are spread over 4 days.

nomena observed in naturally occurring disease. These data are those of Tigertt and Benenson (54) on respiratory Q fever in man. This set of data is of importance in that it demonstrates conclusively that the naturally occurring disease results from a minimal dose, probably of the order of d_0 or less.

A plot of mean incubation period as a function of dose is given in Fig. 39. The incubation period is defined as the time between respiratory challenge and the onset of a persistent temperature above 100 F. The data are meager; for example, for $d/d_0 = 1$, there were only two cases of infection, both with incubation period of 17 days; for other points, there were three or four cases and it was possible to determine a crude value of the standard error of the mean time. Nevertheless,

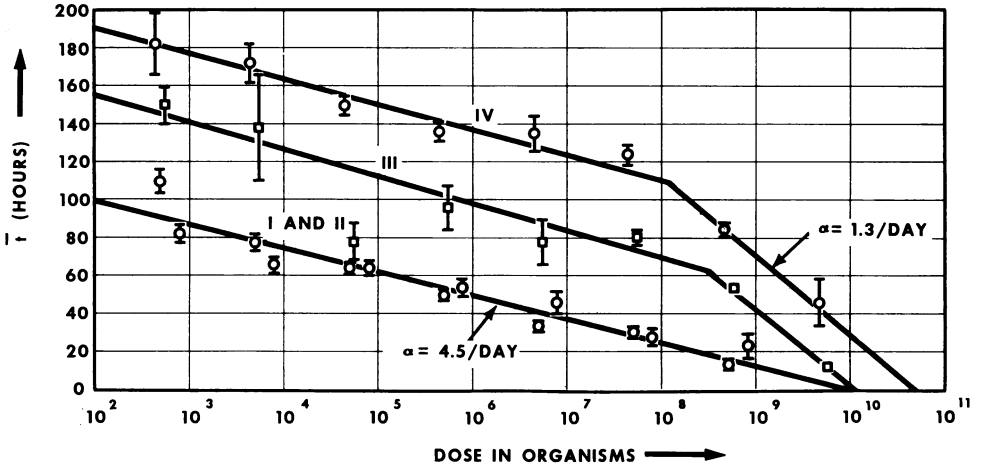

FIG. 35. *Mean time to death of mice infected intraperitoneally with Pasteurella tularensis Church.*

The set of curves in Fig. 36 represents the best detailed agreement of the birth-death model with experiment that we have found.

Figures 37 and 38 show additional examples of observed response-time distributions, together with observed values of $\alpha\sigma$ and skewness suitable for comparison with the predictions of Fig. 28. Figure 37 represents data on tularemia in mice (2), and Fig. 38 shows the rabbit-wart data already discussed in connection with Fig. 33 (10).

As pointed out earlier, the observed values of $\alpha\sigma$ are generally much too large, whereas the values of skewness are in reasonable agreement with prediction.

Comparison with Naturally Occurring Disease

There is one set of data available that permits comparison of the birth-death model with phe-

the data are sufficiently good to obtain a value of $\alpha \approx 1.2$/day, and of $N/d_0 \approx 10^9$.

From these values of α and N/d_0, and Table 1 of the previous paper (52), we can plot the theoretical frequency distribution of incubation periods for $d/d_0 = 1$ (Fig. 40). As indicated in Fig. 24, this same curve will represent closely the distribution for any lower dose.

We also show in Fig. 40 a summary of observations on the incubation period of naturally occurring Q fever, taken from the review by Huebner et al. (29). It will be noted that, typically, the observed times are spread over a wider range than are those predicted by the theory. However, the fact that the shortest observed incubation period is 13 days, whereas Tigertt and Benenson observed one period of 12 days with a dose as low as $d/d_0 = 15$, makes it apparent that the natural infection occurs from challenge with a very low dose.

We offer these data as justification for the hypothesis that naturally occurring respiratory infections arise from doses in the vicinity of d_0 or less and that this fact results in the rather well-defined minimal incubation periods that are observed. This hypothesis needs to be checked for data on respiratory infections other than Q fever.

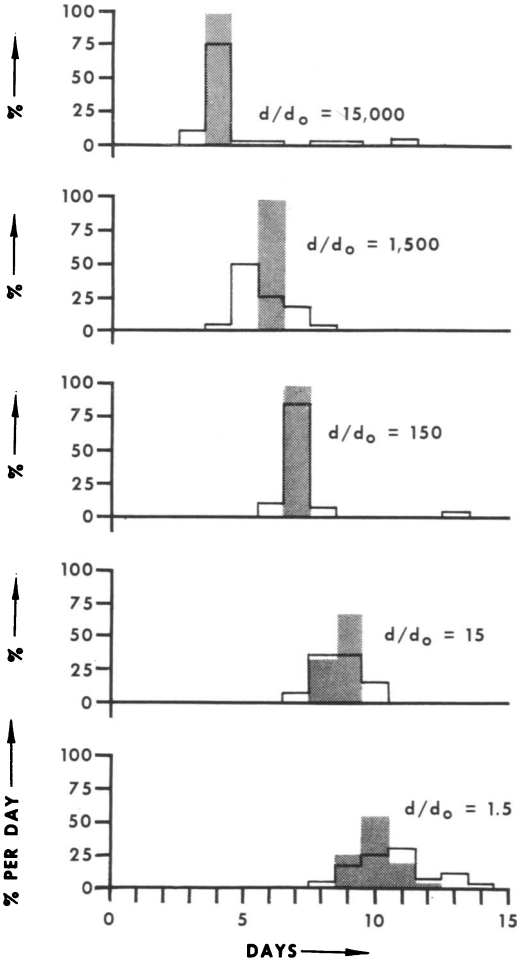

FIG. 36. *Distributions of time to death for guinea pigs inoculated intraperitoneally with Q fever—comparison of experiment (open bars) with model (cross-hatched bars).*

SUGGESTED RESEARCH TOOLS

One of the least-understood periods in the course of infectious disease lies between the initial inoculation with a dose of organisms and the appearance of the first symptoms of disease, or the lack of appearance thereof. In particular, the factors affecting susceptibility and resistance are poorly understood.

Conventional laboratory and statistical techniques have failed to recognize and adjust for host heterogeneity. It is suggested that the detailed study of the reasons for host heterogeneity may give useful clues to the broader area of determination of the factors influencing susceptibility.

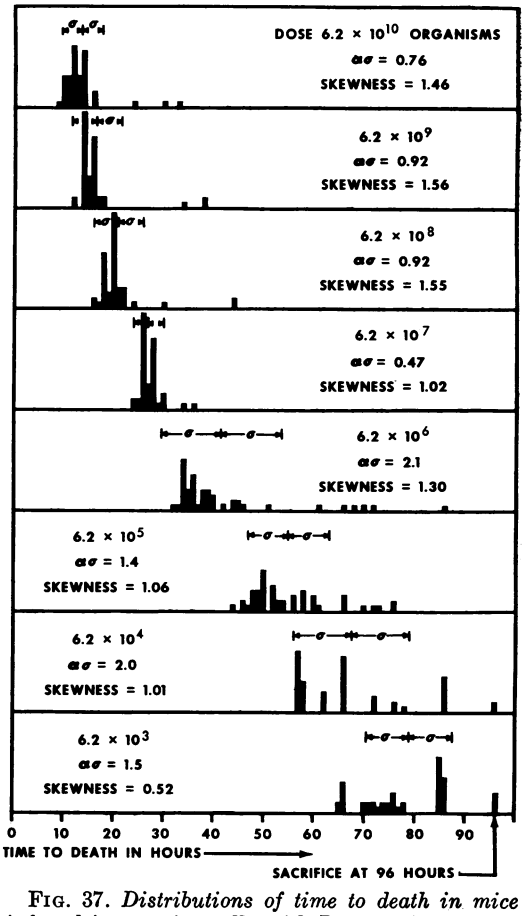

FIG. 37. *Distributions of time to death in mice infected intraperitoneally with Pasteurella tularensis (d_0 = 0.69 organism).*

Research is needed along a variety of lines to identify genetically controlled or physiological factors of defense against infective agents. In this section, we suggest avenues of approach that utilize the analytical techniques described in the preceding sections.

Utilization of "Shelf" Behavior to Study Sensitivity and Resistance Factors

When the response-probability curve has a definite shelf, as in Fig. 41, which repeats the

anthrax curve of Fig. 7, the independent-action model attributes the two-group behavior to a division of the hosts into two groups, irrespective of any heterogeneity there may be in organism behavior.

On any model, it is difficult to attribute a behavior such as that in Fig. 41 to other than host factors. One cannot reasonably attribute this behavior to organism differences. Even if a fraction of the organisms are of enhanced virulence, the number of these virulent organisms increases continuously as we move from left to right, and it seems impossible to account for a response probability that remains constant after the dose of these virulent organisms reaches a certain size, thus producing a shelf. The only reasonable way of accounting for the shelf is the assumption that 65% of the hosts are susceptible and respond to a low dose, whereas the other 35% are resistant and require a high dose. The only other conceivable assumption is the far-fetched one of assuming that 65% of the hosts were properly inoculated in the proper region, and that the inoculum was consistently maladministered in the other 35% of the hosts, for example subcutaneously instead of intraperitoneally and that the subcutaneous lethal dose is higher than the intraperitoneal.

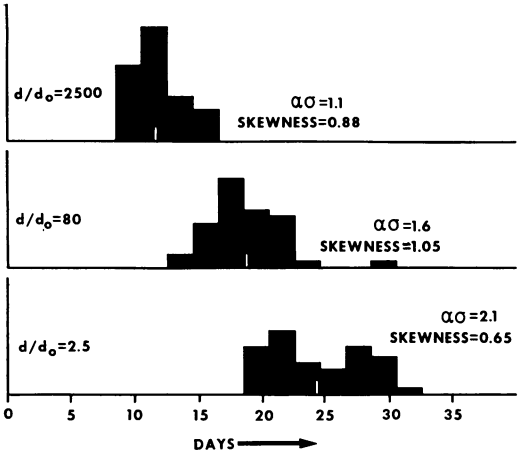

FIG. 38. *Distributions of time to development of warts in rabbits challenged with papilloma virus by skin scarification.*

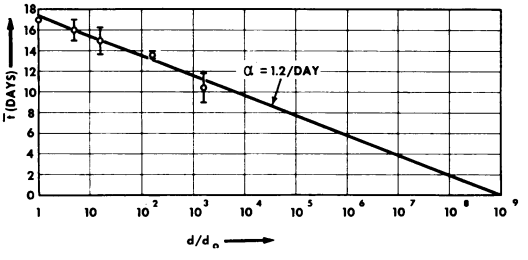

FIG. 39. *Mean incubation time of respiratory Q fever in man.*

If we accept the reality of host differences, then a curve of the type in Fig. 41 gives us the possibility of separating the resistant from the susceptible hosts on the basis of their response to a single selected dose. For example, a dose of 3×10^2 organisms will kill substantially all of the susceptible hosts, whereas substantially all of the resistant hosts will live.

This argument leads to the possibility of determining the host factors that are related to the difference in susceptibility by (i) making individual host measurements prior to inoculation, (ii) carefully labeling the hosts, (iii) subjecting them to challenge at the same selected dose, and later (iv) correlating the response with the measured host characteristics.

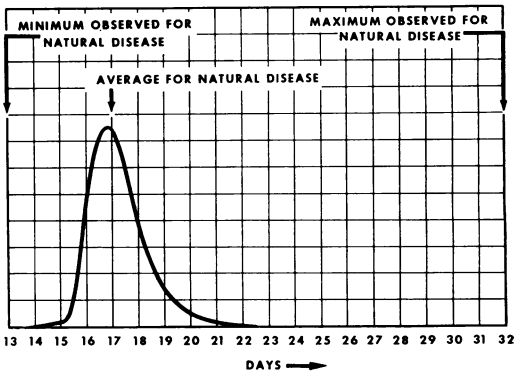

FIG. 40. *Comparison of theoretical incubation-period distribution for $d/d_0 = 1$ with natural observations of Q fever in man.*

It is recommended that the above-described tool be carefully explored as a means of solving the puzzle of resistance and susceptibility frequently observed in apparently homogeneous host groups, and obtaining further insight into the general problem of factors influencing susceptibility.

Utilization of Host Age and Heterogeneity to Study Defense Mechanisms

During the course of this study, we have been impressed with the number of cases in which young animals responded homogeneously and older ones heterogeneously. In Table 4 and Fig. 20, this phenomenon is shown in chick embryos

infected with *Coccidioides immitis*; in Table 3 the same phenomenon is shown to occur in mice challenged by extraneural routes with neurotropic viruses. In general, the change from homogeneity to heterogeneity occurs within a relatively short time interval, e.g., in an interval of 24 to 48 hr for chick embryos. Since an understanding of the factors that influence the variation of susceptibility with age is of fundamental importance to all aspects of infectious diseases, this section will attempt to structure some research problems in this area.

The chick embryo has been a favorite laboratory host for many years, as it is highly susceptible to almost all of the known pathogens. Through the efforts of embryologists, histologists, and biochemists, more is probably known about the chick embryo than about any other host. There has been, however, little effort to marry this vast backlog of information to the events occurring during experimental infections. It is more difficult and challenging aspect. A number of suggestions will be made which we hope will encourage research in this area.

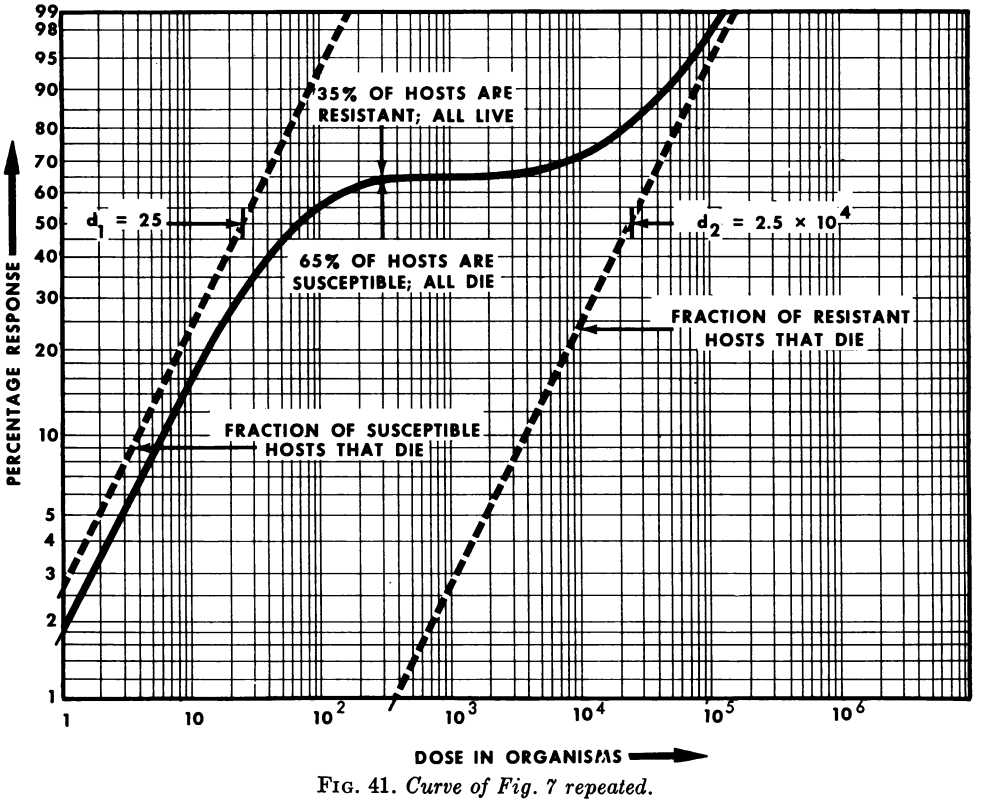

FIG. 41. *Curve of Fig. 7 repeated.*

It has been known for some time that young animals are more susceptible to infection than older ones. This phenomenon is particularly true for viral diseases, as is brought out in the review by Siegel (53). However, research on the problem of susceptibility as a function of age has been hampered by the lack of (i) a technique for identifying host heterogeneity, and (ii) specific experiments to investigate host-defense factors. The first requirement has been partially met by the technique described in the section on the independent-action model for identifying host heterogeneity. The second problem of designing experiments to study host-defense factors is the known, for example, that age of the chick embryo at the time of challenge markedly influences susceptibility. In the case of *Coccidioides immitis*, we noted that embryos up to 7 days of age were homogeneously susceptible to the organism. When challenged at 8 days of age, the hosts were heterogeneous and two groups were identified, one group with increased susceptibility and the other group resistant. By the ninth day, the embryos were almost completely resistant. It is not surprising that susceptibility in the embryo changes within a matter of hours, when one considers that complete embryonic development takes place in about 500 hr. However, of im-

TABLE 9. *Fifty per cent confidence limits (expressed as percentages)*

Size of sample (N)	No. (n) observed to exhibit the characteristic of interest																													
	0		1		2		3		4		5		6		7		8		9		10		11		12		13		14		15	
	P_1	P_2	P_1	P_2	P_1	P_2	P_1	P_2	P_1	P_2	P_1	P_2	P_1	P_2	P_1	P_2	P_1	P_2	P_1	P_2	P_1	P_2	P_1	P_2	P_1	P_2	P_1	P_2	P_1	P_2	P_1	P_2
1	0	75	25	100																										
2	0	50	13	87	50	100																								
3	0	37	9	67	33	90	63	100																						
4	0	29	7	54	24	76	46	93	71	100																				
5	0	24	6	45	19	64	36	81	55	94	76	100																		
6	0	21	5	39	16	55	30	70	45	84	61	95	79	100																
7	0	18	4	34	14	49	25	62	38	75	51	86	66	96	82	100														
8	0	16	4	30	12	43	22	56	33	67	44	78	57	88	70	96	84	100												
9	0	14	3	27	11	39	20	50	29	61	39	71	50	80	61	89	73	97	86	100										
10	0	13	3	25	10	36	18	46	26	56	35	65	44	74	54	82	64	90	75	97	87	100								
11	0	12	3	23	9	33	16	42	24	51	32	60	40	68	49	76	58	84	67	91	77	97	88	100						
12	0	11	2	21	8	30	15	39	22	47	29	55	37	63	45	71	53	78	61	85	70	92	79	98	89	100				
13	0	10	2	19	7	28	13	36	20	44	27	52	34	59	41	66	48	73	56	80	64	87	72	93	81	98	90	100		
14	0	9	2	18	7	26	12	34	18	41	25	48	31	55	38	62	45	69	52	75	59	82	66	88	74	93	82	98	91	100
15	0	9	2	17	6	24	12	32	17	39	23	45	29	52	35	59	41	65	48	71	55	77	61	83	68	88	76	94	83	98	91	100
16	0	8	2	16	6	23	11	30	16	36	22	43	27	49	33	55	39	61	45	67	51	73	57	78	64	84	70	89	77	94	84	98
17	0	8	2	15	6	22	10	28	15	34	20	41	25	46	31	52	36	58	42	64	48	69	54	75	59	80	66	85	72	90	78	94
18	0	7	2	14	5	21	10	27	14	33	19	38	24	44	29	50	34	55	40	60	45	66	50	71	56	76	62	81	67	86	73	90
19	0	7	2	14	5	20	9	25	14	31	18	37	23	42	27	47	32	52	37	58	42	63	48	68	53	73	58	77	63	82	89	86
20	0	7	1	13	5	19	9	24	13	30	17	35	22	40	26	45	31	50	35	55	40	60	45	65	50	69	55	74	60	78	65	83
21	0	6	1	12	5	18	8	23	12	28	16	33	21	38	25	43	29	48	34	53	38	57	43	62	47	66	52	71	57	75	62	79
22	0	6	1	12	4	17	8	22	12	27	16	32	20	37	24	41	28	46	32	50	36	55	41	59	45	64	50	68	54	72	59	76
23	0	6	1	11	4	16	8	21	11	26	15	31	19	35	23	40	27	44	31	48	35	53	39	57	43	61	47	66	52	69	56	73
24	0	6	1	11	4	16	7	20	11	25	14	29	18	34	22	38	25	42	29	46	33	51	37	55	41	59	45	63	49	67	54	71
25	0	5	1	10	4	15	7	20	10	24	14	28	17	32	21	37	24	41	28	45	32	49	36	53	39	57	43	61	47	64	51	68
26	0	5	1	10	4	15	7	19	10	23	13	27	16	31	20	35	23	39	27	43	31	47	34	51	38	55	42	58	45	62	49	66
27	0	5	1	10	4	14	6	18	9	22	13	26	16	30	19	34	23	38	26	42	29	45	33	49	36	53	40	56	44	60	47	64
28	0	5	1	9	3	14	6	18	9	21	12	25	15	29	18	33	22	37	25	40	28	44	32	47	35	51	39	55	42	58	45	61
29	0	5	1	9	3	13	6	17	9	21	12	25	15	28	18	32	21	35	24	39	27	42	31	46	34	49	37	53	40	56	44	60
30	0	5	1	9	3	13	6	16	9	20	11	24	14	27	17	31	20	34	23	38	26	41	30	45	33	48	36	51	39	54	42	58

31	0	4	1	8	3	12	6	16	8	19	11	23	14	26	17	30	20	33	23	37	26	40	29	43	32	46	35	50	38	53	41	56
32	0	4	1	8	3	12	5	15	8	19	11	22	13	26	16	29	19	32	22	35	25	39	28	42	31	45	34	48	37	51	40	54
33	0	4	1	8	3	12	5	15	8	18	10	22	13	25	16	28	18	31	21	34	24	38	27	41	30	44	32	47	35	50	38	53
34	0	4	1	8	3	11	5	15	8	18	10	21	13	24	15	27	18	30	20	34	23	37	26	40	29	43	31	46	34	48	37	51
35	0	4	1	8	3	11	5	14	7	17	10	20	12	24	15	27	17	30	20	33	23	36	25	38	28	41	31	44	33	47	36	50
36	0	4	1	7	3	11	5	14	7	17	9	20	12	23	14	26	17	29	19	32	22	35	24	37	27	40	30	43	32	46	35	49
37	0	4	1	7	3	10	5	13	7	16	9	19	12	22	14	25	16	28	19	31	21	34	24	36	26	39	29	42	31	45	34	47
38	0	4	1	7	3	10	5	13	7	16	9	19	11	22	14	25	16	27	18	30	21	33	23	36	26	38	28	41	31	44	33	46
39	0	3	1	7	2	10	4	13	7	16	9	18	11	21	13	24	15	27	18	29	20	32	23	35	25	37	27	40	30	43	32	45
40	0	3	1	7	2	10	4	12	6	15	8	18	11	21	13	23	15	26	17	29	20	31	22	34	24	36	27	39	29	42	31	44
41	0	3	1	6	2	9	4	12	6	15	8	18	10	20	13	23	15	25	17	28	19	31	21	33	24	36	26	38	28	41	31	43
42	0	3	1	6	2	9	4	12	6	15	8	17	10	20	12	22	14	25	17	27	19	30	21	32	23	35	25	37	28	40	30	42
43	0	3	1	6	2	9	4	12	6	14	8	17	10	19	12	22	14	24	16	27	18	29	20	32	23	34	25	36	27	39	29	41
44	0	3	1	6	2	9	4	11	6	14	8	16	10	19	12	21	14	24	16	26	18	29	20	31	22	33	24	36	26	38	28	40
45	0	3	1	6	2	9	4	11	6	14	8	16	9	18	11	21	13	23	15	26	17	28	19	30	22	33	24	35	26	37	28	39
46	0	3	1	6	2	8	4	11	6	13	7	16	9	18	11	20	13	23	15	25	17	27	19	30	21	32	23	34	25	36	27	39
47	0	3	1	6	2	8	4	11	5	13	7	15	9	18	11	20	13	22	15	25	17	27	19	28	21	31	23	33	25	36	27	38
48	0	3	1	6	2	8	4	10	5	13	7	15	9	17	11	20	13	22	14	24	16	26	18	28	20	31	22	33	24	35	26	37
49	0	3	1	5	2	8	4	10	5	13	7	15	9	17	10	19	12	21	14	24	16	26	18	28	20	30	22	32	24	34	25	36
50	0	3	1	5	2	8	3	10	5	12	7	14	9	17	10	19	12	21	14	23	16	25	17	27	19	29	21	32	23	34	25	36

portance is the identification of the particular changes that take place between the seventh and ninth days, and which make some embryos susceptible and others resistant to the infection. It would appear that a logical attack on this problem would be a comprehensive review of all available data on the chick embryo. Special attention should be paid to anatomical and cellular changes and alterations in biochemistry that occur from day to day. In parallel with this survey, information on the nutritional requirements, biochemistry, and virulence factors of the pathogen should be collected. The analysis of this information would then attempt to relate changes in the developing embryo with specific characteristics of the pathogen. As an example, it is possible that, at a certain age of the embryo, substrates conducive to the growth of the pathogen or for the expression of virulence are altered or disappear so that susceptibility is reduced. Intuitively, one would not expect these alterations to occur simultaneously at exactly the same age of development. Rather, during the transition period between susceptibility and resistance, individual differences could account for the fact that some embryos are sensitive and others are resistant. There is also the strong possibility that all embryos were not hatched at exactly the same time and that this difference could help account for the host heterogeneity observed during the period in which resistance is developing. It is felt that a review of the available data would prevent rediscovery of known information, give clues to mechanisms involved, and aid in the generating of useful hypotheses to be tested in the laboratory.

Tissue culture is an ideal system for studying factors of susceptibility and resistance at the cellular level, especially for viral diseases. If one could demonstrate heterogeneity in tissue cultures infected with viruses, he would have a potentially powerful tool in looking for factors related to susceptibility and resistance. By examining such heterogeneous cultures with biochemical or immunochemical techniques, it may be possible to relate alterations in cell metabolism with resistance. However, in a limited review of the literature, we have found that dose-response studies in tissue culture with viral agents always give a linear plot on the Weibull scale, indicating a homogeneous system. Additional dose-response studies with tissue culture and viruses are needed in the following areas: (i) studies using different strains of cell lines infected with a wide spectrum of viruses; (ii) dose-response data from tissue cultures of different ages at the time of challenge; (iii) use of cell lines from hosts naturally resistant to the viruses.

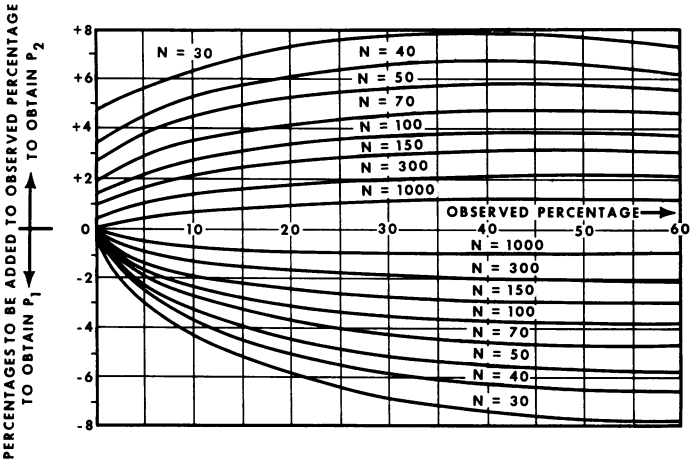

FIG. 42. *Confidence limits (50%) for samples of N items.*

Another important application of tissue culture would be to use tissue cultures derived from hosts of different ages. The suggestion for this program came from the recent investigations of Nir and Goldwasser (42), who observed that the increase of resistance to West Nile virus with age was a general phenomenon, no matter what routes of inoculation were used. It was pointed out in the section on the birth-death model that young mice were susceptible to neurotropic viruses given by extraneural routes; with increasing age, the animals responded heterogeneously until about 40 days of age, when they were completely resistant. The purpose of this suggested program

is to attempt to mimic, in a tissue-culture system, the homogeneity and heterogeneity observed in the intact animal. The first step would be to develop tissue-culture systems from a variety of different tissue sites. These tissues would come from the host at different ages, e.g., from 3-, 25-, 40-, and 200-day-old mice. The next step would be to challenge the tissue system with one of the neurotropic viruses. Dose-response data would be collected and analyzed. Such a study might cast interesting light on the influence of age on susceptibility to viral diseases.

APPENDIX: 50% CONFIDENCE LIMITS

For the small sample sizes usually used in determining response percentages, we have found the 50% confidence limits to give the most useful indication of the statistical accuracy of the observed percentage. For these limits there is at least a 50% chance that the true population percentage lies between the limits, at most a 25% chance that it lies above the upper limit, and at most a 25% chance that it lies below the lower limit. Where the response is 0 or 100%, there is at least a 75% chance that the true percentage lies between the limits.

These limits give a usable indication of the accuracy with which a plotted curve should fit the observed data. It is a "good bet," i.e., there is a better than 50% chance, that the curve will pass between the limits. Use of the more common 95 or 99% confidence limits gives, for small samples, limits so far apart as to be much less useful.

For convenience, we give in Table 9 the 50% confidence limits for a range of small samples. The table is complete up to sample size equal to 30, because the number (n) heading the columns can be either the number that respond or the number that do not respond. Thus, if 10 of 30 respond, we have confidence limits for response of $P_1 = 26$ and $P_2 = 41\%$, as read directly in the column $n = 10$ and the line $N = 30$. On the other hand, if 20 of 30 respond, we note that 10 do not respond, so we have 26 and 41% confidence limits for nonresponse, or 59 and 74% confidence limits for response.

For sample sizes larger than 30, the confidence limits can be obtained from Fig. 42, which shows the percentage to be added to the observed percentage to obtain P_2, or subtracted to obtain P_1, for various sample sizes N.

ACKNOWLEDGMENTS

We wish to express our appreciation to the U.S. Army for assistance rendered and for unpublished data made available during the course of this work. We also thank our colleague, G. Ronald Herd, for his many helpful suggestions and his useful advice.

This work was performed under contract with the U.S. Army.

LITERATURE CITED

1. AINSLEE, D. J. 1952. The growth curve of the Lansing strain of poliomyelitis virus in the central nervous system of the mouse. J. Exp. Med. **95**:1–7.
2. ARMITAGE, P. 1959. An examination of some experimental cancer data in the light of the one-hit theory of infectivity titrations. J. Nat. Cancer Inst. **23**:1313–1330.
3. BANG, F. B. 1948. Studies on New Castle disease virus. I. An evaluation of the method of titration. J. Exp. Med. **88**:233–240.
4. BELL, F. J., C. R. OWEN, AND C. L. LARSON. 1955. Virulence of *Bacterium tularense*. I. A study of the virulence of *Bacterium tularense* in mice, guinea pigs, and rabbits. J. Infect. Dis. **97**:162–166.
5. BERRY, L. J., M. K. DEROPP, M. H. FAIR, AND E. M. SHUR. 1956. Dynamics of bacterial infections in mice under conditions known to alter survival time. J. Infect. Dis. **98**:198–207.
6. BJERKEDAL, T. 1960. Acquisition of resistance in guinea pigs infected with different doses of virulent tubercle bacilli. Amer. J. Hyg. **72**:130–148.
7. BODIAN, D., I. M. MORGAN, AND H. A. HOWE. 1949. Differentiation of types of poliomyelitis viruses. III. The grouping of fourteen strains into three basic immunological types. Amer. J. Hyg. **49**:234–245.
8. BONEZZI, V. G., V. L. CAVALLI, AND G. MAGNI. 1943. Quantitative Untersuchunger über die Virulenz. I. Mitteilung: Eine Virulenzgleichung und ihre biologische Deutung. Zentr. Bakteriol. Parasitenk. Abt. I Orig. **150**:17–25.
9. BRYAN, W. R. 1956. Biological studies on the rous sarcoma virus. IV. Interpretation of tumor-response data involving one inoculation site per chicken. J. Nat. Cancer Inst. **16**:843–863.
10. BRYAN, W. R., AND J. W. BEARD. 1939. Estimation of purified papilloma virus protein by infectivity measurements. J. Infect. Dis. **65**:306–321.
11. BRYAN, W. R., AND J. W. BEARD. 1940. Correlation of frequency of positive inoculation with incubation period and concentration of purified papilloma protein. J. Infect. Dis. **66**:245–253.
12. BRYAN, W. R., AND J. W. BEARD. 1940. Host influence in the characterization of response to the papilloma protein and to vaccinia virus. J. Infect. Dis. **67**:5–24.
13. CAVALLI, V. L., AND G. MAGNI. 1943. Quantitative Untersuchungen über die Virulenz. II. Mitteilung: Die bakteriostatische Wirkung der Sulfanilamide *in vivo*. Zentr. Bakteriol. Parasitenk. Abt. I Orig. **150**:25–32.
14. CROCKER, T. T. 1947. The number of elementary bodies per 50 per cent lethal dose of meningo-pneumonitis virus as determined

by electron microscopic counting. J. Immunol. **73**:1–7.
15. CROCKER, T. T., AND B. M. BENNETT. 1955. The slope assay for measurement of lethal potency of meningo-pneumonitis virus in the chick embryo. J. Immunol. **75**:239–248.
16. DONOVON, J. E., D. HAM, G. M. FUKUI, AND M. J. SURGALLA. 1961. Role of the capsule of *Pasteurella pestis* in bubonic plague in the guinea pig. J. Infect. Dis. **109**:154–157.
17. DUTTON, A. A. C. 1955. The influence of the route of inoculation on lethal infections in mice. Brit. J. Exp. Pathol. **36**:128–136.
18. ECKERT, E. A., D. BEARD, AND J. W. BEARD. 1951. Dose-response relations in experimental transmission of avian erythromyeloblastic leukosis. I. Host response to the virus. J. Nat. Cancer Inst. **12**:447–463.
19. EYLES, D. E., AND N. COLEMAN. 1956. Relationship of size of inoculum to time of death in mice infected with *Toxoplasma gondii*. J. Parasitol. **42**:272–276.
20. FAINE, S. 1957. Virulence in leptospira. II. The growth *in vivo* of virulent *Leptospira icterohaemorrhagiae*. Brit. J. Exp. Pathol. **38**:8–14.
21. FAZEKAS DE ST. GROTH, S., AND P. A. P. MORAN. 1955. Noninfective influenza virus. J. Hyg. **53**:291–296.
22. FENNER, F. 1948. The epizootic behavior of mouse-pox (infectious ectromelia). Brit. J. Exp. Pathol. **29**:69–91.
23. FUKUI, G. M., W. D. LAWTON, W. A. JANSSEN, AND M. G. SURGALLA. 1957. Response of guinea pig lungs to *in vivo* and *in vitro* cultures of *Pasteurella pestis*. J. Infect. Dis. **100**: 103–107.
24. GARD, S. 1940. Encephalomyelitis of mice. II. A method for measurement of virus activity. J. Exp. Med. **72**:69–77.
25. GOGOLAK, F. M. 1953. A quantitative study of the infectivity of murine pneumonitis virus in mice infected in a cloud chamber of improved design. J. Infect. Dis. **92**:240–247.
26. GOLUB, O. J. 1948. A single-dilution method for the estimation of LD_{50} titers of the psittacosis-LGV group of viruses in chick embryos. J. Immunol. **59**:71–82.
27. GÖNNERT, V. R. 1942. Über einige Eigenschaften des Bronchopneumonievirus der Maus. Zentr. Bakteriol. Parasitenk. Abt. I Orig. **148**:331–337.
28. HOFFMAN, J. G., H. L. GOTTZ, M. C. REINHARD, AND S. G. WARNER. 1943. Quantitative determination of the growth of a transplantable mouse adenocarcinoma. Cancer Res. **3**:237–242.
29. HUEBNER, R. J., W. L. JELLISON, AND M. D. BECK. 1949. Q fever—a review of current knowledge. Ann. Intern. Med. **30**:495–509.
30. JUNGEBLUT, C. W., AND M. SANDERS. 1940. Studies of a murine strain of poliomyelitis virus in cotton rats and white mice. J. Exp. Med. **72**:407–435.
31. KJELLÉN, L. 1956. Studies on adenoviruses (APC-RI-ARD) in tissue culture. Correlation between the amount of virus inoculated and the time needed for production of cellular degeneration. Arch. Virusforsch. **7**:110–119.
32. KLIGLER, I. J., AND G. RABINOWITCH. 1927. Susceptibility and resistance to trypanosome infections. III. The relation of dosage to the course of infection. Ann. Trop. Med. Parasitol. **21**:375–380.
33. LENNETTE, E. H., AND H. KOPROWSKI. 1944. Influence of age on the susceptiblity of mice to infection with certain neurotropic viruses. J. Immunol. **49**:175–191.
34. LEY, H. L., JR., J. E. SMADEL, F. H. DIERCKS, AND P. Y. PATERSON. 1952. Immunization against scrub typhus. V. The infective dose of *Rickettsia tsutsugamushi* for men and mice. Amer. J. Hyg. **56**:313–319.
35. LINCOLN, R. E., AND I. A. DEARMON, JR. 1959. Homogeneity of response of mouse and guinea pig strains to virulence tests with *Bacillus anthracis* and *Pasteurella tularensis*. J. Bacteriol. **78**:640–650.
36. MAGNUSON, H. J., H. EAGLE, AND R. FLEISCHMAN. 1948. The minimal infectious inoculum of *Spirochaeta pallida* (Nichols strain) and a consideration of its rates of multiplication *in vitro*. Amer. J. Syph. Gonor. Vener. Dis. **32**:1–19.
37. MAGNUSON, H. J., AND G. J. ROSENAU. 1948. The rate of development and degree of acquired immunity in experimental syphilis. Amer. J. Syph. Gonor. Vener. Dis. **32**:418–436.
38. MAGNUSON, H. J., E. W. THOMAS, S. OLANSKY, B. I. KAPLAN, L. DEMELLO, AND J. C. CUTLER. 1956. Inoculation syphilis in human volunteers. Medicine **35**:33–82.
39. MARSHALL, R. G., AND P. J. GERONE. 1961. Susceptibility of suckling mice to a variola virus. J. Bacteriol. **82**:15–19.
40. MEYNELL, G. G., AND E. W. MEYNELL. 1958. The growth of microorganisms *in vivo* with particular reference to the relation between dose and latent period. J. Hyg. **56**:323–346.
41. MIMS, C. A. 1956. Rift valley fever virus in mice. III. Further quantitative features of the infective process. Brit. J. Exp. Pathol. **37**:120–128.
42. NIR, Y. R., AND R. GOLDWASSER. 1961. Biological characteristics of some of the Arbor viruses *in vivo* and *in vitro*. II. Multiplication and cytopathogenicity of West Nile virus in kidney tissue cultures from various animals compared with the susceptibility of the animals *in vivo*. Amer. J. Hyg. **73**:297–302.
43. ORMSBEE, R. A., D. B. LACKMAN, AND E. G. PICKENS. 1951. Relationships among complement-fixing values, infectious end points, and death curves in experimental *Coxiella burnetii* infection. J. Immunol. **67**:257–263.
44. PARKER, R. F., L. H. BRONSON, AND R. H.

GREEN. 1945. Further studies of the infectious unit of vaccinia. J. Exp. Med. **74**:263–281.

45. PIKE, R. M., AND G. M. MACKENZIE. 1940. Virulence of Salmonella typhimurium. I. Analysis of experimental infection in mice with strains of high and low virulence. J. Bacteriol. **40**:171–195.
46. PRIGGE, R. 1941. Experimentelle Untersuchungen zur Chemotherapie der Tuberkulose. II. Mitteilung. Kling. Wochschr. **20**:633–657.
47. PRINCE, A. M., A. S. LITTELL, AND H. S. GINSBERG. 1957. Methods for quantitative bioassay of Ehrlich Ascites-tumor cells. J. Nat. Cancer Inst. **18**:487–506.
48. REINHARD, M. C., H. L. GOETZ, AND S. WARNER. 1945. Further studies on the quantitative determination of the growth of a transplantable mouse adenocarcinoma. Cancer Res. **5**:102–106.
49. ROESSLER, W. G., J. L. CONVERSE, AND J. A. GEATING. 1961. Virulence assay of *Coccidiodes immitis* in embryonated eggs. J. Bacteriol. **81**:226–232.
50. SAATY, T. L. 1961. Some stochastic processes with absorbing barriers. J. Roy. Statist. Soc. Ser. B **23**:319–334.
51. SHEPARD, C. C. 1960. The experimental disease that follows the injection of human leprosy bacillus into footpads of mice. J. Exp. Med. **112**:445–454.
52. SHORTLEY, G. 1965. A stochastic model for distributions of biological response times. Biometrics (*in press*).
53. SIEGEL, M. M. 1952. Influence of age on susceptibility to virus infections with particular reference to laboratory animals. Ann. Rev. Microbiol. **6**:247–279.
54. TIGERTT, W. D., AND A. S. BENENSON. 1956. Studies on Q fever in man. Trans. Assoc. Amer. Physicians **68**:98–104.
55. TIGERTT, W. D., A. S. BENENSON, AND W. S. GOCHENOUR. 1961. Airborne Q fever. Bacteriol. Rev. **25**:285–293.
56. WEISS, E. 1950. Multiplication of the agent of feline pneumonitis in the yolk sacs of dead chick embryos. J. Infect. Dis. **86**:27–32.
57. YOUMANS, G. P., AND A. S. YOUMANS. 1951. The relation between the size of the infecting dose of tubercle bacilli and the survival time of mice. Amer. Rev. Tuberc. **64**:534–540.